

STABILITY ANALYSIS OF LINE PATTERNS OF AN ANISOTROPIC INTERACTION MODEL

José A. Carrillo^{*} Bertram Düring[†] Lisa Maria Kreusser[‡] Carola-Bibiane Schönlieb[§]

Abstract. Motivated by the formation of fingerprint patterns we consider a class of interacting particle models with anisotropic, repulsive-attractive interaction forces whose orientations depend on an underlying tensor field. This class of models can be regarded as a generalization of a gradient flow of a nonlocal interaction potential which has a local repulsion and a long-range attraction structure. In addition, the underlying tensor field introduces an anisotropy leading to complex patterns which do not occur in isotropic models. Central to this pattern formation are straight line patterns. We show that there exists a preferred direction of straight lines, i.e. straight vertical lines can be stable for sufficiently many particles, while other rotations of the straight lines are unstable steady states, both for a sufficiently large number of particles and in the continuum limit. For straight vertical lines we consider specific force coefficients for the stability analysis of steady states, show that stability can be achieved for exponentially decaying force coefficients for a sufficiently large number of particles and relate these results to the Kücken-Champod model for simulating fingerprint patterns. The mathematical analysis of the steady states is completed with numerical results.

AMSC: 35B36, 35Q92, 70F10, 70F45, 82C22

Keywords: Aggregation, swarming, pattern formation, dynamical systems.

1. INTRODUCTION

Mathematical models for biological aggregation describing the collective behaviour of large numbers of individuals have given us many tools to understand pattern formation in nature. Typical examples include models for explaining the complex phenomena observed in swarms of insects, flocks of birds, schools of fish or colonies of bacteria see for instance [7, 8, 12, 18, 24, 32, 33, 34, 35, 37, 45, 48, 49]. Some continuum models have been derived from individual based descriptions [53, 14, 15, 16, 40, 52, 56, 13], see also the reviews [25, 41], leading to an understanding of the stability of patterns at different levels [11, 42, 1, 27, 26].

A key feature of many of these models is that the communication between individuals takes place at different scales, i.e. each individual can interact not only with its neighbours but also with individuals further away. This can be described by short- and long-range interactions [8, 37, 45]. In most models the interactions are assumed to be *isotropic* for simplicity. However, pattern formation in nature is usually *anisotropic* [6]. Motivated by the simulation of fingerprint patterns we consider a class of interacting particle models with *anisotropic* interaction forces in this paper. In particular, these anisotropic interaction models capture important swarming

^{*}Department of Mathematics, Imperial College London, London SW7 2AZ, United Kingdom; *carrillo@imperial.ac.uk*

[†]Department of Mathematics, University of Sussex, Pevensey II, Brighton BN1 9QH, United Kingdom; *b.during@sussex.ac.uk*

[‡]Department of Applied Mathematics and Theoretical Physics (DAMTP), University of Cambridge, Wilberforce Road, Cambridge CB3 0WA, United Kingdom; *L.M.Kreusser@damtp.cam.ac.uk*

[§]Department of Applied Mathematics and Theoretical Physics (DAMTP), University of Cambridge, Wilberforce Road, Cambridge CB3 0WA, United Kingdom; *C.B.Schoenlieb@damtp.cam.ac.uk*

behaviours, neglected in the simplified isotropic interaction model, such as anisotropic steady states.

The simplest form of isotropic interaction models is based on radial interaction potentials [4]. In this case one can consider the stationary points of the N -particle interaction energy

$$E(x_1, \dots, x_N) = \frac{1}{2N^2} \sum_{\substack{j,k=1 \\ k \neq j}}^N W(x_j - x_k).$$

Here, $W(d) = \bar{W}(|d|)$ denotes the radially symmetric interaction potential and $x_j = x_j(t) \in \mathbb{R}^n$ for $j = 1, \dots, N$ are the positions of the particles at time $t \geq 0$ [11, 42]. One can easily show that the associated gradient flow reads:

$$\frac{dx_j}{dt} = \frac{1}{N} \sum_{\substack{k=1 \\ k \neq j}}^N F(x_j - x_k), \quad (1.1)$$

where $F(x_j - x_k)$ is a conservative force, aligned along the distance vector $x_j - x_k$ with $F(d) = -\nabla W(d)$. In many biological applications the number of interacting particles is large and one may consider the underlying continuum formulation of (1.1), which is known as the aggregation equation [9, 11, 42] and of the form

$$\rho_t + \nabla \cdot (\rho u) = 0, \quad u = -\nabla W * \rho, \quad (1.2)$$

where $u = u(t, x)$ is the macroscopic velocity field and $\rho = \rho(t, x)$ denotes the density of particles at location $x \in \mathbb{R}^n$ at time $t > 0$. The aggregation equation (1.2) has been studied extensively recently, mainly in terms of its gradient flow structure [2, 29, 30, 44, 54], the blow-up dynamics for fully attractive potentials [9, 10, 21, 28], and the rich variety of steady states for repulsive-attractive potentials [3, 4, 5, 8, 10, 19, 20, 22, 23, 38, 39, 50, 55, 56, 27, 26, 31].

In biological applications, the interactions determined by the force F , or equivalently the interaction potential W , are usually described by short-range repulsion, preventing collisions between the individuals, as well as long-range attraction, keeping the swarm cohesive [46, 47]. In this case, the associated radially symmetric potentials \bar{W} first decrease and then increase as a function of the radius. Due to the repulsive forces these potentials lead to possibly more steady states than the purely attractive potentials. In particular, these repulsive-attractive potentials can be considered as a minimal model for pattern formation in large systems of individuals [4, 41] and the references therein.

Pattern formation in multiple dimensions is studied in [11, 42, 55, 56, 26] for repulsive-attractive potentials. The instabilities of the sphere and ring solutions are studied in [11, 55, 56]. The linear stability of ring equilibria is analysed and conditions on the potential are derived to classify the different instabilities. A numerical study of the N -particle interaction model for specific repulsion-attraction potentials is also performed in [11, 42] leading to a wide range of radially symmetric patterns such as rings, annuli and uniform circular patches, as well as more complex patterns. Based on this analysis the stability of flock solutions and mill rings in the associated second-order model can be studied, see [1] and [27] for the linear and nonlinear stability of flocks, respectively.

In this work, we consider a generalization of the particle model (1.1) by introducing an anisotropy given by a tensor field T . This leads to an extended particle model of the form

$$\frac{dx_j}{dt} = \frac{1}{N} \sum_{\substack{k=1 \\ k \neq j}}^N F(x_j - x_k, T(x_j)) \quad (1.3)$$

where we prescribe initial data $x_j(0) = x_j^{in}$, $j = 1, \dots, N$, for given scalars x_j^{in} , $j = 1, \dots, N$. A special instance of this model has been introduced in [43] for simulating fingerprint patterns.

The particle model in its general form (1.3) has been studied in [17, 36]. Here, the positions of each of the N particles at time t are denoted by $x_j = x_j(t) \in \mathbb{T}^2$, $j = 1, \dots, N$, where \mathbb{T}^2 denotes the two-dimensional torus, and $F(x_j - x_k, T(x_j))$ denotes the total force that particle k exerts on particle j subject to an underlying stress tensor field $T(x_j)$ at x_j , given by

$$T(x) := \chi s(x) \otimes s(x) + l(x) \otimes l(x) \in \mathbb{R}^{2,2} \quad (1.4)$$

for orthonormal vector fields $s = s(x)$ and $l = l(x) \in \mathbb{R}^2$ and $\chi \in [0, 1]$. The parameter χ introduces an anisotropy in the direction s in the definition of the tensor field.

For purely repulsive forces along s and short-range repulsive, long-range attractive forces along l the numerical simulations in [17] suggest that straight vertical line patterns formed by the interacting particles at positions x_j are stable for a certain spatially homogeneous tensor field, specified later. In this paper, we want to rigorously study this empirical observation by providing a linear stability analysis of such patterns where particles distribute equidistantly along straight lines.

The stability analysis of steady states of the particle model (1.3) is important for understanding the robustness of the patterns that arise from applying (1.3) for numerical simulation, for instance as for its originally intended application to fingerprint simulation in [43]. Indeed, in what follows, we will show that for spatially homogeneous tensor fields T the solution formed by a number of vertical straight lines (referred to as ridges) is a stationary solution, whereas ridge bifurcations, i.e. a single ridge dividing into two ridges as typically appearing in fingerprint patterns, is not.

The aim of this paper is to prove that sufficiently large numbers of particles distributed equidistantly along straight vertical lines are stable steady states to the particle model (1.3) for short-range repulsive, long-range attractive forces along l and purely repulsive forces along s . All other rotations of straight lines are unstable steady states for this choice of force coefficients for a sufficiently large number of particles and for the continuum limit. We focus on this very simple class of steady states as a first step towards understanding stable formations that can be achieved by model (1.3). Note that the continuum straight line is a steady state of the associated continuum model

$$\partial_t \rho(t, x) + \nabla_x \cdot [\rho(t, x) (F(\cdot, T(x)) * \rho(t, \cdot))(x)] = 0 \quad \text{in } \mathbb{R}_+ \times \mathbb{R}^2,$$

see [17], but its asymptotic stability cannot be concluded from the linear stability analysis for finitely many particles.

The paper is organized as follows. In Section 2 we describe a general formulation of an anisotropic interaction model, based on the model proposed by Kücken and Champod [43]. Section 3 is devoted to a high-wave number stability analysis of line patterns for the continuum limit $N \rightarrow \infty$, including vertical, horizontal and rotated straight lines for spatially homogeneous tensor fields. Due to the instability of arbitrary rotations except for vertical straight lines for the considered tensor field we focus on the stability analysis of straight vertical lines for particular forces for any $N \in \mathbb{N}$ in Section 4. Section 5 illustrates the form of the steady states in case the derived stability conditions are not satisfied.

2. DESCRIPTION OF THE MODEL

In this section, we describe a general formulation of the anisotropic microscopic model (1.3) and relate it to the Kücken-Champod particle model [43]. Kücken and Champod consider the particle model (1.3) where the total force F is given by

$$F(d(x_j, x_k), T(x_j)) = F_A(d(x_j, x_k), T(x_j)) + F_R(d(x_j, x_k)) \quad (2.1)$$

for the distance vector $d(x_j, x_k) = x_j - x_k \in \mathbb{R}^2$. Here, F_R denotes the repulsion force that particle k exerts on particle j and F_A is the attraction force particle k exerts on particle j . The

repulsion and attraction forces are of the form

$$F_R(d = d(x_j, x_k)) = f_R(|d|)d \quad (2.2)$$

and

$$F_A(d = d(x_j, x_k), T(x_j)) = f_A(|d|)T(x_j)d, \quad (2.3)$$

respectively, where, again, $d = d(x_j, x_k) = x_j - x_k \in \mathbb{R}^2$. Note that the repulsion and attraction forces are radially symmetric. The direction of the interaction forces is determined by the parameter $\chi \in [0, 1]$ in the definition of T .

The coefficient function f_R of the repulsion force F_R (2.2) in the Kücken-Champod model (1.3) is given by

$$f_R(|d|) = (\alpha|d|^2 + \beta) \exp(-e_R|d|) \quad (2.4)$$

for $d \in \mathbb{R}^2$ and nonnegative parameters α, β and e_R . The coefficient function f_A of the attraction force (2.3) is given by

$$f_A(|d|) = -\gamma|d| \exp(-e_A|d|) \quad (2.5)$$

for $d \in \mathbb{R}^2$ and nonnegative constants γ and e_A . To be as close as possible to the work by Kücken and Champod [43] we assume that the total force (2.1) exhibits short-range repulsion and long-range attraction along l and one can choose the parameters as:

$$\alpha = 270, \quad \beta = 0.1, \quad \gamma = 35, \quad e_A = 95, \quad e_R = 100, \quad \chi \in [0, 1] \quad (2.6)$$

as proposed in [17] for the particle model (1.3) on the torus \mathbb{T}^2 .

In the sequel, we consider a more general form of the total force (2.1), given by

$$F(d = d(x_j, x_k), T(x_j)) = f_s(|d|)(s(x_j) \cdot d)s(x_j) + f_l(|d|)(l(x_j) \cdot d)l(x_j), \quad (2.7)$$

where the total force is decomposed into forces along direction s and direction l . In particular, the force coefficients in the Kücken-Champod model (1.3) with repulsive and attractive forces F_R and F_A in (2.2) and (2.3), respectively, can be recovered for

$$f_l(|d|) = f_A(|d|) + f_R(|d|) \quad \text{and} \quad f_s(|d|) = \chi f_A(|d|) + f_R(|d|).$$

Since a steady state of the particle model (1.3) for any spatially homogeneous tensor field \tilde{T} can be regarded as a coordinate transform of the steady state of the particle model (1.3) for the tensor field T , see [17] for details, we restrict ourselves to the study of steady states for the spatially homogeneous tensor field T given by the orthonormal vectors $s = (0, 1)$ and $l = (1, 0)$, i.e.

$$T = \begin{pmatrix} 1 & 0 \\ 0 & \chi \end{pmatrix}. \quad (2.8)$$

The total force in the Kücken-Champod model (2.1) and the generalised total force (2.7) reduce to

$$F(d) = \begin{pmatrix} (f_A(|d|) + f_R(|d|)) d_1 \\ (\chi f_A(|d|) + f_R(|d|)) d_2 \end{pmatrix} \quad (2.9)$$

and

$$F(d) = \begin{pmatrix} f_l(|d|)d_1 \\ f_s(|d|)d_2 \end{pmatrix} \quad \text{for } d = (d_1, d_2), \quad (2.10)$$

respectively, for the spatially homogeneous tensor field T in (2.8).

The coefficient functions (2.4) and (2.5) for the repulsion and attraction forces (2.2) and (2.3) as well as the coefficient functions along $s = (0, 1)$ and $l = (1, 0)$ in the Kücken-Champod model (1.3) are plotted in Figure 1 for the parameters in (2.6). Note that repulsive force coefficients are positive and the attractive force coefficients are negative. Repulsion dominates for short distances along l to prevent the collision of particles. Besides, the total force exhibits long-range

attraction along l whose absolute value decreases with the distance between particles. Along s the particles are purely repulsive for $\chi = 0.2$ and the repulsion force gets weaker for longer distances.

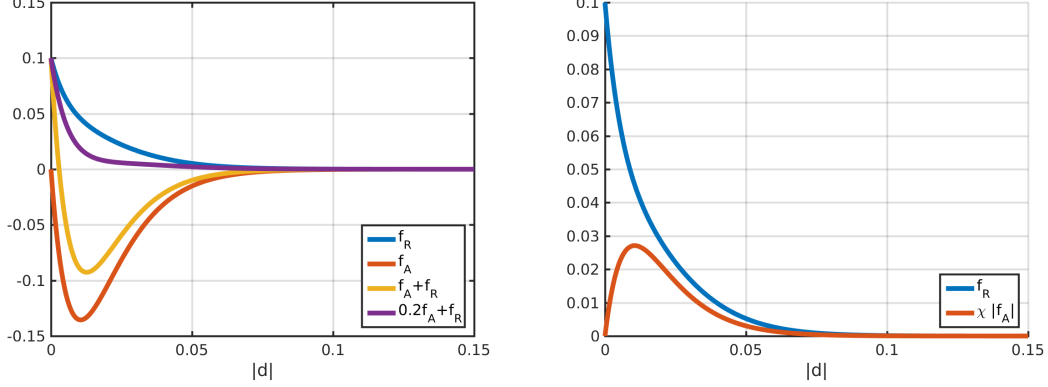


FIGURE 1. Coefficients f_R in (2.4) and f_A in (2.5) of repulsion force (2.2) and attraction force (2.3), respectively, as well as the force coefficients along $s = (0, 1)$ and $l = (1, 0)$ (i.e. $f_A + f_R$ and $0.2f_A + f_R$) for parameter values in (2.6)

In the sequel, we consider the particle model (1.3) for $x_j \in \mathbb{T}^2$ which is equivalent to considering the unit square $[0, 1]^2$ with periodic boundary conditions and a cutoff radius of $R_c = 0.5$ for the force coefficients, i.e. for a force coefficient f given by a piecewise C^1 function we consider the piecewise C^1 function

$$\begin{cases} f, & |d| \leq R_c, \\ 0, & |d| > R_c. \end{cases}$$

Motivated by this, we also consider smaller values of the cutoff radius $R_c \in (0, 0.5]$. Note that we do not require continuity at the cutoff. However, this is in analogy to the notion of cutoff. These assumptions are not restrictive and by rescaling in time our analysis extends to any domain $[0, d]^2$ with a cutoff radius $R_c \in (0, \frac{d}{2}]$ for $d \in \mathbb{R}_+$.

3. STABILITY/INSTABILITY OF STRAIGHT LINES

In this section we assume that the total force F , defined in (2.9), can be described by a short-range repulsive, long-range attractive force coefficient f_l along l and a purely repulsive force coefficient f_s along s . Motivated by this we require in the sequel:

Assumption 3.1 *Let f_l, f_s restricted to $[0, R_c)$ be continuously differentiable functions on $[0, R_c)$. Let f_s be purely repulsive, i.e. $f_s \geq 0$ with $f_s(s) > 0$ for $s \in [0, R_c)$, implying $\int_0^{R_c} f_s ds > 0$. Further let f_l be short-range repulsive, long-range attractive, implying $f_l(R_c) \leq 0$.*

As shown in [17], it is sufficient to restrict ourselves to the spatially homogeneous tensor field T with $s = (0, 1)$ and $l = (1, 0)$ for the analysis of steady states with general spatially homogeneous tensor fields in the sequel.

3.1. Straight line. In this section we consider line patterns as steady states which were observed in the numerical simulations in [17]. For $x_j, j = 1, \dots, N$, evolving according to the particle model (1.3), we have

$$\frac{d}{dt} \sum_{j=1}^N x_j = 0,$$

implying that the centre of mass is conserved. Hence, we can assume without loss of generality that the centre of mass is at the origin. By identifying \mathbb{R}^2 with \mathbb{C} , we make the ansatz

$$\bar{x}_k = \frac{k}{N} \exp(i\vartheta) \ell(\vartheta), \quad k = 1, \dots, N. \quad (3.1)$$

Here, ϑ denotes the angle of rotation. The length of the line pattern is denoted by $\ell = \ell(\vartheta) > 0$ and can be regarded as a multiplicative factor with $\ell(0) = \ell(\frac{\pi}{2}) = 1$ and $\ell(\frac{\pi}{4}) = \ell(\frac{3\pi}{4}) = \sqrt{2}$. Note that it is sufficient to restrict ourselves to $\vartheta \in [0, \pi)$ since ansatz (3.1) for ϑ and $\vartheta + k\pi$ with $k \in \mathbb{Z}$ leads to the same solution. Depending on the choice of ϑ ansatz (3.1) might lead to multiple windings on the torus \mathbb{T}^2 . To guarantee that ansatz (3.1) satisfies the periodic boundary conditions, we require that the winding number of the straight lines in (3.1) is a natural number and hence we can restrict ourselves to ansatz (3.1) on the torus \mathbb{T}^2 for $\vartheta \in \mathcal{A}$ where

$$\begin{aligned} \mathcal{A} := & \left\{ 0, \frac{\pi}{4}, \frac{\pi}{2}, \frac{3\pi}{4} \right\} \cup \left\{ \psi \in \left(0, \frac{\pi}{4} \right) \cup \left(\frac{3\pi}{4}, \pi \right) : \cot(\psi) \in \mathbb{Z} \right\} \\ & \cup \left\{ \psi \in \left(\frac{\pi}{4}, \frac{3\pi}{4} \right) : \tan(\psi) \in \mathbb{Z} \right\}. \end{aligned} \quad (3.2)$$

Note that considering the torus \mathbb{T}^2 as the domain, i.e. the unit square with periodic boundary conditions, is not restrictive due to the discussion in Section 2.

For a single vertical straight line we have $\vartheta = \frac{\pi}{2}$ and ansatz (3.1) reduces to

$$\bar{x}_k = \frac{k}{N} i, \quad k = 1, \dots, N, \quad (3.3)$$

and for a horizontal line with $\vartheta = 0$ we have

$$\bar{x}_k = \frac{k}{N}, \quad k = 1, \dots, N. \quad (3.4)$$

Note that the winding number is one for (3.1) with $\vartheta \in \{0, \frac{\pi}{4}, \frac{\pi}{2}, \frac{3\pi}{4}\}$, while the winding number is larger than one for $\vartheta \in \mathcal{A} \setminus \{0, \frac{\pi}{4}, \frac{\pi}{2}, \frac{3\pi}{4}\}$. Translations of the ansatz (3.1) result in steady states with a non-zero centre of mass. Besides, parallel equidistant straight line patterns, obtained from considering (3.1) for a fixed rotation angle (3.2) and different translations, also lead to steady states.

For equilibria $\bar{x}_j, j = 1, \dots, N$, to the particle model (1.3) we require that

$$\frac{1}{N} \sum_{\substack{k=1 \\ k \neq j}}^N F(\bar{x}_j - \bar{x}_k, T) = 0 \quad \text{for all } j = 1, \dots, N.$$

Since we consider periodic boundary conditions and the particles are uniformly distributed along straight lines by ansatz (3.1), it is sufficient for a steady state to require that

$$\sum_{k=1}^{N-1} F(\bar{x}_N - \bar{x}_k, T) = 0. \quad (3.5)$$

Note that $F(\bar{x}_N - \bar{x}_k, T) = -F(\bar{x}_N - \bar{x}_{N-k}, T)$ for $k = 1, \dots, \lceil N/2 \rceil - 1$ and for N even we have $F(\bar{x}_N - \bar{x}_{N/2}, T) = 0$ by the definition of the total force (2.7). Hence, (3.5) is satisfied for the ansatz (3.1) for $\vartheta \in \mathcal{A}$, provided the length $\ell(\vartheta)$ of the lines is set appropriately on \mathbb{T}^2 .

3.2. Stability conditions. In this section we derive stability conditions for equilibria of the particle model (1.3), based on a linearised stability analysis.

Proposition 3.2 *For finite $N \in \mathbb{N}$, the steady state $\bar{x}_j, j = 1, \dots, N$, of the particle model (1.3) is asymptotically stable if the eigenvalues λ of the stability matrix*

$$M = M(j, m) = \begin{pmatrix} I_1(j, m) & I_2(j, m) \end{pmatrix} \in \mathbb{C}^{2,2} \quad (3.6)$$

with

$$\begin{aligned}
I_1(j, m) &= \frac{1}{N} \sum_{k \neq j} (1 - \exp(im(\phi_k - \phi_j))) \frac{\partial F}{\partial d_1}(\bar{x}_j - \bar{x}_k) \\
&= \frac{1}{N} \sum_{k \neq j} \left(1 - \exp\left(\frac{2\pi im(k-j)}{N}\right) \right) \frac{\partial F}{\partial d_1}(\bar{x}_j - \bar{x}_k) \\
I_2(j, m) &= \frac{1}{N} \sum_{k \neq j} (1 - \exp(im(\phi_k - \phi_j))) \frac{\partial F}{\partial d_2}(\bar{x}_j - \bar{x}_k) \\
&= \frac{1}{N} \sum_{k \neq j} \left(1 - \exp\left(\frac{2\pi im(k-j)}{N}\right) \right) \frac{\partial F}{\partial d_2}(\bar{x}_j - \bar{x}_k)
\end{aligned} \tag{3.7}$$

for $j = 1, \dots, N$ and $m = 1, \dots, N$ satisfy $\Re(\lambda) < 0$ for all $j = 1, \dots, N$ and $m = 1, \dots, N-1$.

Proof. Let \bar{x}_j , $j = 1, \dots, N$, denote a steady state of (1.3). We define the perturbation $g_j = g_j(t)$, $h_j = h_j(t) \in \mathbb{R}$ of \bar{x}_j by

$$x_j = \bar{x}_j + \begin{pmatrix} g_j \\ h_j \end{pmatrix}, \quad j = 1, \dots, N.$$

Linearising (1.3) around the steady state \bar{x}_j gives

$$\frac{d}{dt} \begin{pmatrix} g_j \\ h_j \end{pmatrix} = \frac{1}{N} \sum_{k \neq j} (g_j - g_k) \frac{\partial F}{\partial d_1}(\bar{x}_j - \bar{x}_k) + \frac{1}{N} \sum_{k \neq j} (h_j - h_k) \frac{\partial F}{\partial d_2}(\bar{x}_j - \bar{x}_k). \tag{3.8}$$

We choose the ansatz functions

$$g_j = \zeta_g (\exp(im\phi_j) + \exp(-im\phi_j)), \quad h_j = \zeta_h (\exp(im\phi_j) + \exp(-im\phi_j)), \\ j = 1, \dots, N, \quad m = 1, \dots, N,$$

where $\zeta_g = \zeta_g(t)$, $\zeta_h = \zeta_h(t)$ and $\phi_j = \frac{2\pi j}{N}$. Note that $g_j, h_j \in \mathbb{R}$ for all $j = 1, \dots, N$ and

$$\sum_{j=1}^N \exp(im\phi_j) = \sum_{j=1}^N \left(\exp\left(\frac{2\pi im}{N}\right) \right)^j = \begin{cases} 0, & m = 1, \dots, N-1, \\ N, & m = N, \end{cases}$$

since ϕ_j are the roots of $r^N = 1$ and

$$\sum_{j=0}^{N-1} r^j = \frac{1 - r^N}{1 - r}.$$

This implies

$$\sum_{j=1}^N g_j(t) = \sum_{j=1}^N h_j(t) = \begin{cases} 0, & m = 1, \dots, N-1, \\ N, & m = N, \end{cases}$$

for all times $t \geq 0$, i.e. the centre of mass of the perturbations g_j, h_j is preserved. We have

$$g_j - g_k = \zeta_g (\exp(im\phi_j) + \exp(-im\phi_j)) (1 - \exp(im(\phi_k - \phi_j))), \\ h_j - h_k = \zeta_h (\exp(im\phi_j) + \exp(-im\phi_j)) (1 - \exp(im(\phi_k - \phi_j))).$$

Plugging this into (3.8) and collecting like terms in $\exp(im\phi_j), \exp(-im\phi_j)$ results in

$$\begin{aligned}
\frac{d}{dt} \begin{pmatrix} \zeta_g \\ \zeta_h \end{pmatrix} &= \frac{\zeta_g}{N} \sum_{k \neq j} (1 - \exp(im(\phi_k - \phi_j))) \frac{\partial F}{\partial d_1}(\bar{x}_j - \bar{x}_k) \\
&\quad + \frac{\zeta_h}{N} \sum_{k \neq j} (1 - \exp(im(\phi_k - \phi_j))) \frac{\partial F}{\partial d_2}(\bar{x}_j - \bar{x}_k),
\end{aligned}$$

i.e.

$$\frac{d}{dt} \begin{pmatrix} \zeta_g \\ \zeta_h \end{pmatrix} = M \begin{pmatrix} \zeta_g \\ \zeta_h \end{pmatrix}, \quad (3.9)$$

where the stability matrix M is defined in (3.6). The ansatz $\zeta_g = \xi_g \exp(\lambda t)$, $\zeta_h = \xi_h \exp(\lambda t)$ solves the system (3.9) for any eigenvalue λ of the stability matrix $M = M(j, m)$. Note that the stability matrix M is the zero matrix for $m = N$ and any $j = 1, \dots, N$. Hence, we have $\lambda = 0$ for $m = N$ and all $j = 1, \dots, N$, corresponding to translations along the vertical and horizontal axis. Thus, the straight line $\bar{x}_j, j = 1, \dots, N$, is stable if $\Re(\lambda) < 0$ for any $j = 1, \dots, N$ and $m = 1, \dots, N - 1$. \square

3.3. Stability of a single vertical straight line. To study the stability of a single vertical straight line of the form (3.3) we determine the eigenvalues of the stability matrix (3.6) and derive stability conditions for steady states $\bar{x}_j, j = 1, \dots, N$, satisfying (3.5). In the continuum limit $N \rightarrow \infty$ the steady state condition (3.5) becomes

$$\int_{-0.5}^{0.5} F((0, s), T) ds = 0.$$

Introducing a cutoff radius $R_c \in (0, 0.5]$ it is sufficient to require

$$\int_{-R_c}^{R_c} F((0, s), T) ds = 0 \quad (3.10)$$

for equilibria. This condition is clearly satisfied for forces of the form (2.9).

Theorem 3.3 *For finite $N \in \mathbb{N}$, the single vertical straight line (3.3) is an asymptotically stable steady state of the particle model (1.3) with total force (2.9) if $\Re(\lambda_{i,N}(m)) < 0$ for $i = 1, 2$ and all $m = 1, \dots, N - 1$ where the eigenvalues $\lambda_{i,N} = \lambda_{i,N}(m)$ of the stability matrix (3.6) are given by*

$$\begin{aligned} \lambda_{1,N}(m) &= \frac{1}{N} \sum_{k=1}^N f_l(|d_{Nk}|) \left(1 - \exp\left(\frac{2\pi i m k}{N}\right) \right), \\ \lambda_{2,N}(m) &= \frac{1}{N} \sum_{k=1}^N (f_s(|d_{Nk}|) + f'_s(|d_{Nk}|)|d_{Nk}|) \left(1 - \exp\left(\frac{2\pi i m k}{N}\right) \right) \end{aligned} \quad (3.11)$$

with

$$d_{Nk} = \bar{x}_N - \bar{x}_k = \begin{pmatrix} 0 \\ \frac{N-k}{N} \end{pmatrix}$$

on the torus \mathbb{T}^2 . Denoting the cutoff radius by $R_c \in (0, 0.5]$, steady states satisfy the steady state condition (3.10) in the continuum limit $N \rightarrow \infty$. The steady state in the continuum limit $N \rightarrow \infty$ is unstable if $\Re(\lambda_i(m)) > 0$ for some $m \in \mathbb{N}$ and some $i \in \{1, 2\}$ where the eigenvalues $\lambda_i = \lambda_i(m), i = 1, 2$, of the stability matrix (3.6) are given by

$$\begin{aligned} \lambda_1(m) &= \int_{-R_c}^{R_c} f_l(s) (1 - \exp(-2\pi i m s)) ds, \\ \lambda_2(m) &= \int_{-R_c}^{R_c} (f_s(s) + f'_s(s)|s|) (1 - \exp(-2\pi i m s)) ds. \end{aligned} \quad (3.12)$$

In particular,

$$\begin{aligned} \Re(\lambda_1)(m) &= 2 \int_0^{R_c} f_l(s) (1 - \cos(-2\pi m s)) ds, \\ \Re(\lambda_2)(m) &= 2 \int_0^{R_c} (f_s(s) + f'_s(s)s) (1 - \cos(-2\pi m s)) ds. \end{aligned} \quad (3.13)$$

Proof. The derivatives of the total force (2.9) are given by

$$\frac{\partial F}{\partial d_1}(d) = \begin{pmatrix} f_l(|d|) + f'_l(|d|)\frac{d_1^2}{|d|} \\ f'_s(|d|)\frac{d_1 d_2}{|d|} \end{pmatrix}, \quad \frac{\partial F}{\partial d_2}(d) = \begin{pmatrix} f'_l(|d|)\frac{d_1 d_2}{|d|} \\ f_s(|d|) + f'_s(|d|)\frac{d_2^2}{|d|} \end{pmatrix} \quad (3.14)$$

for $d = (d_1, d_2)$ for the spatially homogeneous tensor field T , defined by $s = (0, 1)$ and $l = (1, 0)$. Using the ansatz (3.3) for a single vertical straight line, we obtain:

$$\begin{aligned} \frac{\partial F}{\partial d_1}(d_{jk}) &= \begin{pmatrix} f_l(|d_{jk}|) \\ 0 \end{pmatrix}, \\ \frac{\partial F}{\partial d_2}(d_{jk}) &= \begin{pmatrix} 0 \\ f_s(|d_{jk}|) + f'_s(|d_{jk}|)|d_{jk}| \end{pmatrix}. \end{aligned} \quad (3.15)$$

Since the particles along the straight vertical line are indistinguishable, it suffices to consider $j = N$ and the entries (3.7) of the stability matrix (3.6) are given by

$$\begin{aligned} I_1(m) &= \frac{1}{N} \sum_{k=1}^N \left(1 - \exp\left(\frac{2\pi i m k}{N}\right) \right) \frac{\partial F}{\partial d_1}(d_{Nk}), \\ I_2(m) &= \frac{1}{N} \sum_{k=1}^N \left(1 - \exp\left(\frac{2\pi i m k}{N}\right) \right) \frac{\partial F}{\partial d_2}(d_{Nk}), \end{aligned} \quad (3.16)$$

where the derivatives of the forces are given by (3.15). Note that the stability matrix (3.6) is a diagonal matrix whose eigenvalues are given by the non-trivial entries in (3.16). Since the sums in (3.16) are Riemannian sums we can pass to the continuum limit $N \rightarrow \infty$. Note that the distance vectors $d_{Nk}, k = 1, \dots, N$, appear in the entries of the stability matrix (3.16). Because of the periodic boundary condition we consider the domain of integration $[0.5, 1.5]$ for passing to the limit $N \rightarrow \infty$ in (3.16), followed by a change of variables. This results in

$$\begin{aligned} I_k(m) &= \int_{0.5}^{1.5} \frac{\partial F}{\partial d_k}((0, 1-s)) (1 - \exp(2\pi i m s)) ds \\ &= \int_{-0.5}^{0.5} \frac{\partial F}{\partial d_k}((0, s)) (1 - \exp(-2\pi i m s)) ds \end{aligned}$$

for $k = 1, 2$ and all $m \in \mathbb{N}$. Clearly the stability matrix (3.6) is again a diagonal matrix and the eigenvalues $\lambda_k = \lambda_k(m), k = 1, 2$, in (3.12) are the diagonal entries of the stability matrix (3.6). \square

Remark 3.4 In Theorem 3.3 we study the stability of the straight vertical line for the dynamical system (1.3) for a finite number of particles N . Note that we cannot conclude stability/instability if $\Re(\lambda_i(m)) \leq 0$ for $i = 1, 2$ and all $m = 1, \dots, N-1$. By the assumptions on the force coefficients f_s, f_l in Assumption 3.1 we can pass to the continuum limit $N \rightarrow \infty$ in the definition of the eigenvalues of the stability matrix and study the stability of the steady states of the particle model (1.3) in the continuum limit $N \rightarrow \infty$. If there exists $m \in \mathbb{N}$ for some $i \in \{1, 2\}$ such that $\Re(\lambda_i(m)) > 0$, then the steady state is unstable in the continuum limit. However, if $\Re(\lambda_i(m)) \leq 0$ for $i \in \{1, 2\}$ and all $m \in \mathbb{N}$ stability/instability of the steady state cannot be concluded since it is difficult to give general conditions for $\Re(\lambda_i(m)) \rightarrow \sigma$ as $m \rightarrow \infty$ with $\sigma = 0$ or $\sigma \in \mathbb{R} \setminus \{0\}$. If $\sigma = 0$, we cannot say anything about the stability/instability of the steady state in the continuum setting, see also similar discussions for the stability/instability of Delta-rings in the continuum setting in [51] and the discussion after Theorem 2.1 in [11]. In particular, linear stability for any $N \in \mathbb{N}$ is not sufficient to conclude stability in the continuum setting.

Note that the asymmetry in the definition of the eigenvalues (3.13) is due to the asymmetric steady states in (3.3). For $f = f_s = f_l$ the total force in (2.9) simplifies to $F(d) = f(|d|)d$ for

$d = (d_1, d_2) \in \mathbb{R}^2$. The gradient of $F = (F_1, F_2)$ is a symmetric matrix by (3.14) and hence the eigenvalues of the stability matrix are real in this case. Since

$$\frac{\partial F_1}{\partial d_2} = \frac{\partial F_2}{\partial d_1}$$

there exists a radially symmetric potential $W(d) = w(|d|)$ such that $F = -\nabla W$. Hence, the stability conditions can be derived in terms of the potential w and we have

$$\text{trace}(\nabla F(d)) = f'(|d|)|d| + 2f(|d|) = -\Delta w(|d|) = \lambda_1 + \lambda_2.$$

For $f_s = f_l$ and a symmetric steady state with respect to the coordinate axes, i.e. $\bar{x}_j = (\bar{x}_{j_1}, \bar{x}_{j_2})$ with $\bar{x}_{j_1} = \bar{x}_{j_2}$, this leads to identical conditions for both eigenvalues λ_k , $k = 1, 2$. For the analysis of these symmetric steady states, however, it is helpful to consider an appropriate coordinate system such as polar coordinates for ring steady states as in [11].

Note that the stability conditions for steady states depend on the choice of the coordinate system. Considering derivatives with respect to the coordinate axes as in (3.14) seems to be the natural choice for straight line patterns, in contrast to polar coordinates as in [11].

In the sequel, we investigate the high-wave number stability of straight line patterns for the particle model (1.3), i.e. the stability of straight vertical lines as $m \rightarrow \infty$. This can be studied by considering the limit $m \rightarrow \infty$ of the eigenvalues (3.12) of the stability matrix (3.6) associated with the dynamical system (3.9).

Proposition 3.5 *Suppose that the coefficient functions f_s and f_l restricted to $[0, R_c)$ are in $C^1([0, R_c))$ with f'_s, f'_l integrable and $f_s \geq 0$. The condition*

$$\int_0^{R_c} f_l(s) ds \leq 0 \quad \text{and} \quad f_s(R_c) = 0 \quad (3.17)$$

is necessary for the high-wave number stability of the single straight vertical line (3.3), i.e. (3.17) is necessary for the stability of the straight vertical line for any $N \in \mathbb{N}$ and in the continuum limit $N \rightarrow \infty$.

Proof. The eigenvalues (3.12) of the stability matrix (3.6) associated with the equilibrium of a single vertical straight line are of the form

$$\begin{aligned} \lambda(m) &= \int_{-R_c}^{R_c} f(|s|)(1 - \exp(-2\pi i m s)) ds \\ &= 2 \int_0^{R_c} f(s) ds - \frac{1}{2\pi i m} \int_{-R_c}^{R_c} f'(|s|) \exp(-2\pi i m s) ds \\ &\quad + \frac{1}{2\pi i m} f(R_c) (\exp(-2\pi m R_c) - \exp(2\pi m R_c)) \end{aligned}$$

for a function $f: \mathbb{R}_+ \rightarrow \mathbb{R}$. For high-wave number stability we require

$$\int_0^{R_c} f(s) ds \leq 0 \quad \text{and} \quad |f'| \text{ is integrable on } [0, R_c].$$

Then, using the definition of the eigenvalues (3.12) this leads to the conditions

$$\int_0^{R_c} f_l(s) ds \leq 0 \quad \text{and} \quad \int_0^{R_c} f_s(s) + f'_s(s)s ds \leq 0. \quad (3.18)$$

Integration by parts of the second condition in (3.18) leads to $f_s(R_c) \leq 0$ and the conditions in (3.17) result from f_s being repulsive, i.e. $f_s \geq 0$. \square

Remark 3.6 *The necessary condition $f_s(R_c) = 0$ in (3.17) for a stable straight vertical line is equivalent to the eigenvalue associated with f_s to be equal to zero in the high-wave number limit. Hence, stability/instability of straight vertical lines cannot be concluded in the continuum limit $N \rightarrow \infty$ from the linear stability analysis.*

The first condition in (3.17) implies that the total attractive force over its entire range is larger than the total repulsive force along l . The second condition in (3.17) implies that for high-wave stability we require the total force at the cutoff radius R_c should not be repulsive along s .

In comparison with the high-wave number conditions in (3.18) in the proof of Proposition 3.5 the integrands for the stability conditions are multiplied by a factor

$$\Re(1 - \exp(-2\pi i m s)) = 1 - \cos(2\pi m s) \in [0, 2].$$

Even if the necessary conditions for high-wave number stability (3.17) are satisfied, this does not guarantee that $\Re(\lambda_1(m)), \Re(\lambda_2(m)) \leq 0$ for all $m \in \mathbb{N}$ and hence necessary stability conditions for the single vertical straight line might not be satisfied for all $m \in \mathbb{N}$.

The general stability conditions for straight vertical lines can be obtained from the real parts of the eigenvalues (3.12) of the stability matrix (3.6). The conditions (3.17) suggest that stability of the straight line is possible for particular force coefficient choices. This will be investigated in Section 4.

Remark 3.7 Note that the force coefficients f_R and f_A in the Kücken-Champod model are defined in (2.5), respectively. Since $f_l = f_A + f_R$ and $f_s = \chi f_A + f_R$ for a parameter $\chi \in [0, 1]$ such that $f_s > 0$ we obtain for the real parts of the eigenvalues of the stability matrix (3.6) in the Kücken-Champod model with total force (2.1) and the spatially homogeneous tensor field T in (2.8)

$$\begin{aligned} \Re(\lambda_1(m)) &= 2 \int_0^{R_c} (f_A(s) + f_R(s)) (1 - \cos(-2\pi m s)) ds, \\ \Re(\lambda_2(m)) &= 2 \int_0^{R_c} (\chi f_A(s) + f_R(s) + \chi f'_A(s)s + f'_R(s)s) (1 - \cos(-2\pi m s)) ds \end{aligned} \quad (3.19)$$

due to the real parts of the eigenvalues in (3.13). The necessary stability condition (3.17) implies that $f_s(R_c) = \chi f_A(R_c) + f_R(R_c) = 0$. However, this cannot be satisfied for any choice of parameters in the definition of the force coefficients (2.4) and (2.5) in the Kücken-Champod model. For e_R and e_A sufficiently large, the value of $\chi f_A(R_c) + f_R(R_c)$ is a small positive number. Hence, one may replace the force coefficients f_R and f_A in (2.4) and (2.5) by

$$\bar{f}_R(|d|) = f_R(|d|) - f_R(R_c), \quad \bar{f}_A(|d|) = f_A(|d|) - f_A(R_c).$$

This changes the force coefficients f_R and f_A only slightly for e_R and e_A sufficiently large, but we obtain $\chi f_A(R_c) + f_R(R_c) = 0$, i.e. the necessary condition (3.17) for high-wave number stability of a straight vertical line is satisfied.

3.4. Instability of a single horizontal straight line. In this section we investigate the stability of a single horizontal straight line given by the ansatz (3.4) which follows from (3.1) with $\vartheta = 0$.

Theorem 3.8 For $N \in \mathbb{N}$ sufficiently large and in the continuum limit $N \rightarrow \infty$ the single horizontal straight line (3.4) is an unstable steady state to the particle model (1.3) for any choice of force coefficients f_s and f_l of the total force (2.7), provided the total force is purely repulsive along s .

Proof. For a single horizontal straight line, we have

$$d_{jk} = \bar{x}_j - \bar{x}_k = \begin{pmatrix} \frac{j-k}{N} \\ 0 \end{pmatrix}$$

and the derivatives of the total force are given by

$$\begin{aligned}\frac{\partial}{\partial d_1} F(d_{jk}) &= \begin{pmatrix} f_l(|d_{jk}|) + f'_l(|d_{jk}|)|d_{jk}| \\ 0 \end{pmatrix}, \\ \frac{\partial}{\partial d_2} F(d_{jk}) &= \begin{pmatrix} 0 \\ f_s(|d_{jk}|) \end{pmatrix}.\end{aligned}$$

Similar as in Section 3.3 one can show that the eigenvalues $\lambda_1 = \lambda_1(m)$, $\lambda_2 = \lambda_2(m)$ of the stability matrix (3.6) are given by

$$\begin{aligned}\lambda_1(m) &= 2 \int_0^{R_c} (f_l(s) + f'_l(s)s) (1 - \exp(-2\pi i m s)) ds, \\ \lambda_2(m) &= 2 \int_0^{R_c} f_s(s) (1 - \exp(-2\pi i m s)) ds\end{aligned}$$

for a cutoff radius $R_c \in (0, 0.5]$. For high-wave number stability we require

$$f_l(R_c) = \frac{1}{R_c} \int_0^{R_c} f_l(s) + f'_l(s)s ds \leq 0 \quad \text{and} \quad \int_0^{R_c} f_s(s) ds \leq 0.$$

The forces are assumed to be purely repulsive along s , i.e. $f_s > 0$ on $[0, R_c)$, implying

$$\int_0^{R_c} f_s(s) ds > 0.$$

Hence, the single horizontal straight line is high-wave unstable. \square

3.5. Instability of rotated straight line patterns. In this section we consider the ansatz (3.1) where the angle of rotation ϑ satisfies (3.2), resulting in rotated straight line patterns. The entries of the stability matrix (3.6) are given by

$$\begin{aligned}I_1(m) &= 2 \int_0^{R_c} \frac{\partial F}{\partial d_1} ((s \cos(\vartheta), s \sin(\vartheta))) (1 - \exp(-2\pi i m s)) ds, \\ I_2(m) &= 2 \int_0^{R_c} \frac{\partial F}{\partial d_2} ((s \cos(\vartheta), s \sin(\vartheta))) (1 - \exp(-2\pi i m s)) ds,\end{aligned}$$

where the derivatives of the total force can easily be determined by

$$\frac{\partial}{\partial d_1} F(d) = \begin{pmatrix} f_l(|d|) + f'_l(|d|) \frac{d_1^2}{|d|} \\ f'_s(|d|) \frac{d_1 d_2}{|d|} \end{pmatrix}, \quad \frac{\partial}{\partial d_2} F(d) = \begin{pmatrix} f'_l(|d|) \frac{d_1 d_2}{|d|} \\ f_s(|d|) + f'_s(|d|) \frac{d_2^2}{|d|} \end{pmatrix}$$

with the cutoff radius $R_c \in (0, 0.5]$. In particular, the stability matrix (3.6) is no longer a diagonal matrix in general. To show that the rotated straight line pattern is unstable for $\vartheta \in (0, \pi) \setminus \frac{\pi}{2}$ for $N \in \mathbb{N}$ sufficiently large and in the continuum limit $N \rightarrow \infty$, it is sufficient to consider the high frequency wave limit and show high-wave number instability. Denoting the entries of I_k by I_{k1} and I_{k2} for $k = 1, 2$ with $M = (I_1, I_2)$ the high-frequency limit leads to

$$\begin{aligned}I_{11} &= 2 \int_0^{R_c} f_l(s) ds + 2 \int_0^{R_c} f'_l(s)s \cos^2(\vartheta) ds, & I_{12} &= 2 \int_0^{R_c} f'_s(s)s \sin(\vartheta) \cos(\vartheta) ds, \\ I_{21} &= 2 \int_0^{R_c} f'_l(s)s \sin(\vartheta) \cos(\vartheta) ds, & I_{22} &= 2 \int_0^{R_c} f_s(s) ds + 2 \int_0^{R_c} f'_s(s)s \sin^2(\vartheta) ds.\end{aligned} \tag{3.20}$$

Here, $I_{12} = I_{21} = 0$ for $\vartheta = 0$ and $\vartheta = \frac{\pi}{2}$, i.e. for the straight horizontal and the straight vertical line, respectively. Hence, the eigenvalues of the stability matrix are given by I_{11} and I_{22} in this case whose value are given by

$$I_{11} = 2R_c f_l(R_c), \quad I_{22} = 2 \int_0^{R_c} f_s(s) ds$$

for $\vartheta = 0$ and

$$I_{11} = 2 \int_0^{R_c} f_l(s) ds, \quad I_{22} = 2R_c f_s(R_c)$$

for $\vartheta = \frac{\pi}{2}$. This leads to the necessary conditions for high-wave number stability for $\vartheta = \frac{\pi}{2}$ in (3.17), while due to Assumption 3.1 we obtain instability of the straight horizontal line.

Note that for any $\vartheta \in [0, \pi)$ the eigenvalues $\lambda_k, k = 1, 2$, are either real or complex conjugated and thus the sum and the product of λ_k are real. The condition $\Re(\lambda_k) \leq 0, k = 1, 2$, is equivalent to $\text{trace}(M) = \lambda_1 + \lambda_2 \leq 0$ and $\det(M) = \lambda_1 \lambda_2 \geq 0$. Hence, we require for the stability of the rotated straight line:

$$I_{11} + I_{22} \leq 0 \quad \text{and} \quad I_{11}I_{22} - I_{12}I_{21} \geq 0. \quad (3.21)$$

For showing the instability of the rotated straight line with angle of rotation $\vartheta \in (0, \pi) \setminus \frac{\pi}{2}$ we show that the conditions in (3.21) cannot be satisfied simultaneously in this case.

Theorem 3.9 *For $N \in \mathbb{N}$ sufficiently large and in the continuum limit $N \rightarrow \infty$, the single straight line (3.1) where the angle of rotation $\vartheta \in (0, \pi) \setminus \frac{\pi}{2}$ satisfies (3.2) is an unstable steady state to the particle model (1.3) for any force coefficients f_s and f_l satisfying the general conditions for force coefficients in Assumption 3.1 and the conditions in (3.17).*

Proof. Note that we have

$$\int_0^{R_c} f'_s(s) s \sin^2(\vartheta) ds = \sin^2(\vartheta) \left(f_s(R_c) R_c - \int_0^{R_c} f_s(s) ds \right)$$

by integration by parts. For $\vartheta = 0$ and $f_l(R_c) = 0$ we have

$$I_{11} + I_{22} = 2R_c f_l(R_c) + 2 \int_0^{R_c} f_s(s) ds > 0,$$

while for $\vartheta = \frac{\pi}{2}$ we have

$$I_{11} + I_{22} = 2R_c f_s(R_c) + 2 \int_0^{R_c} f_l(s) ds \leq 0$$

by (3.17). Hence, there exist $\vartheta_1 \in (0, \frac{\pi}{2})$ and $\vartheta_2 \in (\frac{\pi}{2}, \pi)$ such that $I_{11} + I_{22} > 0$ on $(0, \vartheta_1) \cup (\vartheta_2, \pi)$ and hence stability can only be possible on $[\vartheta_1, \vartheta_2]$. For the determinant of the stability matrix (3.6) with entries I_{ij} in (3.20) we obtain

$$\begin{aligned} I_{11}I_{22} - I_{12}I_{21} &= 4 \int_0^{R_c} f_l(s) ds \int_0^{R_c} f_s(s) ds + 4 \int_0^{R_c} f_l(s) ds \int_0^{R_c} f'_s(s) s \sin^2(\vartheta) ds \\ &\quad + 4 \int_0^{R_c} f_s(s) ds \int_0^{R_c} f'_l(s) s \cos^2(\vartheta) ds \\ &= 4f_s(R_c)R_c \sin^2(\vartheta) \int_0^{R_c} f_l(s) ds + 4f_l(R_c)R_c \cos^2(\vartheta) \int_0^{R_c} f_s(s) ds \\ &= 4f_l(R_c)R_c \cos^2(\vartheta) \int_0^{R_c} f_s(s) ds \end{aligned}$$

by the conditions in (3.17). Note that the right-hand side is zero for $\vartheta = \frac{\pi}{2}$ for any choice of $f_l(R_c) \leq 0$ as in Assumption 3.1. For $\vartheta \in (0, \pi) \setminus \frac{\pi}{2}$, however, the right-hand side can either be negative or equal to zero depending on the value of $f_l(R_c)$. If $f_l(R_c) < 0$ this immediately implies that the right-hand side is negative for $\vartheta \in (0, \pi) \setminus \frac{\pi}{2}$ and hence $I_{11}I_{22} - I_{12}I_{21} < 0$. Thus, one eigenvalue is positive in the high-wave number limit and the rotated straight line is unstable. \square

4. STABILITY OF VERTICAL LINES FOR PARTICULAR FORCE COEFFICIENTS

We have investigated the high-wave number stability in Section 3. Since only vertical straight lines for the considered spatially homogeneous tensor field T in (2.8) can lead to stable steady states for any $N \in \mathbb{N}$ we restrict ourselves to vertical straight lines in the sequel. As a next step towards proving stability we consider the stability for fixed modes $m \in \mathbb{N}$ now.

Due to the form of the eigenvalues in (3.12) no general stability result for the single straight vertical line for the particle system (1.3) with arbitrary force coefficients f_s and f_l can be derived. Thus, additional assumptions on the force coefficients are necessary.

4.1. Linear force coefficients. To study the stability of the single straight vertical line for any $N \in \mathbb{N}$ we consider linear force coefficients satisfying Assumption 3.1. For linear force coefficients Assumption 3.1 leads to the following conditions:

Assumption 4.1 *We assume that the force coefficients are linear, i.e.*

$$f_l(|d|) = a_l|d| + b_l \quad \text{and} \quad f_s(|d|) = a_s|d| + b_s \quad (4.1)$$

for constants a_l, a_s, b_l and b_s . Since f_l and f_s are short-range repulsive, we require

$$b_l > 0, \quad b_s > 0.$$

Besides, for physically realistic force coefficients the absolute values of f_l and f_s are decaying, i.e.

$$a_l < 0, \quad a_s < 0.$$

Remark 4.2 *Note that the modelling assumptions in Assumptions 3.1 and 4.1 are satisfied for linear repulsive and attractive force coefficients f_R and f_A of the repulsion and attraction forces (2.2) and (2.3), respectively. For*

$$f_R(|d|) = a_R|d| + b_R \quad \text{and} \quad f_A(|d|) = a_A|d| + b_A \quad (4.2)$$

for constants a_A, a_R, b_A and b_R , we require

$$f_R \geq 0 \quad \text{and} \quad f_A \leq 0,$$

implying

$$a_R s + b_R \geq 0 \quad \text{and} \quad a_A s + b_A \leq 0 \quad \text{for } s \in [0, R_c], \quad (4.3)$$

and in particular

$$b_R > 0 \quad \text{and} \quad b_A < 0. \quad (4.4)$$

For realistic interaction force coefficients f_R and f_A we assume that their absolute values decrease as the distance between the particles increases, implying

$$a_R < 0 \quad \text{and} \quad a_A > 0 \quad (4.5)$$

by the definition of f_R and f_A in (4.1) and by the condition on b_R and b_A in (4.4). Combining the assumptions on a_A, a_R in (4.5) and b_A, b_R in (4.4) condition (4.3) reduces to

$$a_R R_c + b_R \geq 0 \quad \text{and} \quad a_A R_c + b_A \leq 0. \quad (4.6)$$

Further we assume that $f_A + f_R$ is short-range repulsive, long-range attractive, i.e.

$$(f_A + f_R)(0) = b_A + b_R > 0, \quad (f_A + f_R)(R_c) = (a_A + a_R)R_c + b_A + b_R < 0,$$

implying

$$b_A + b_R > 0 \quad \text{and} \quad a_A + a_R < 0. \quad (4.7)$$

Note that the force coefficient $\chi f_A + f_R$ is purely repulsive along s if $\chi \in [0, 1]$ is sufficiently small since f_R is purely repulsive. Note that (4.7) implies

$$\chi a_A + a_R < 0, \quad \chi b_A + b_R > 0 \quad \text{for all } \chi \in [0, 1] \quad (4.8)$$

by the positivity of b_R and by the negativity of a_R in (4.4) and (4.5). Since

$$f_l(|d|) = f_A(|d|) + f_R(|d|) = (a_A + a_R)|d| + b_A + b_R$$

and

$$f_s(|d|) = \chi f_A(|d|) + f_R(|d|) = (\chi a_A + a_R)|d| + \chi b_A + b_R,$$

we have

$$a_l = a_A + a_R < 0, \quad a_s = \chi a_A + a_R < 0, \quad b_l = b_A + b_R > 0, \quad b_s = \chi b_A + b_R > 0$$

as in Assumption 4.1.

For investigating the stability of the straight line for any $N \in \mathbb{N}$, we consider the real parts of the eigenvalues in (3.13), i.e.

$$\begin{aligned} \Re(\lambda_1(m)) &= 2 \int_0^{R_c} f_l(s) (1 - \cos(-2\pi ms)) ds, \\ \Re(\lambda_2(m)) &= 2 \int_0^{R_c} (f_s(s) + f'_s(s)s) (1 - \cos(-2\pi ms)) ds. \end{aligned}$$

Note that the coefficient functions of the integrands in the definition of the eigenvalues are given by

$$f_l(s) = a_l s + b_l, \quad f_s(s) + f'_s(s)s = 2a_s s + b_s$$

with $a_l, a_s < 0$, $b_l, b_s > 0$ by Assumption 4.1. Hence, we have linear functions of the form $f: [0, R_c] \rightarrow \mathbb{R}, s \mapsto as + b$ for constants $a < 0$ and $b > 0$. The integrals in (3.12) for $\Re(\lambda_k)$, $k = 1, 2$, are of the form

$$\Re(\lambda_k(m)) = 2 \int_0^{R_c} (a_k s + b_k) (1 - \cos(2\pi ms)) ds, \quad (4.9)$$

where

$$a_1 = a_l, \quad a_2 = 2a_s, \quad b_1 = b_l, \quad b_2 = b_s. \quad (4.10)$$

For ease of notation we drop the indices of a_k and b_k in the sequel. Note that

$$\begin{aligned} &\int_0^{R_c} (as + b) (1 - \cos(2\pi ms)) ds \\ &= \frac{2\pi m (\pi m R_c (a R_c + 2b) - (a R_c + b) \sin(2\pi m R_c)) - a \cos(2\pi m R_c) + a}{4\pi^2 m^2}. \end{aligned} \quad (4.11)$$

In the limit $m \rightarrow \infty$, all terms in the second line of (4.11) vanish except for the first term and since $R_c > 0$, we require

$$a \leq -b \frac{2}{R_c} \quad (4.12)$$

for high-wave number stability which is consistent with the necessary condition for high-wave number stability in Proposition 3.5 for arbitrary force coefficients f_R and f_A . Since $R_c \in (0, 0.5]$ and $b > 0$, (4.12) implies that $a < 0$ is necessary for high-wave number stability. Hence, we can assume

$$a < 0 \quad \text{and} \quad b > 0$$

in the sequel.

Lemma 4.3 *Let $b > 0$ and $R_c \in (0, 0.5]$. Set*

$$\begin{aligned} g(m) &:= 2\pi m (\pi m R_c^2 - R_c \sin(2\pi m R_c)) + 1 - \cos(2\pi m R_c), \\ h(m) &:= 2\pi m (2\pi m R_c - \sin(2\pi m R_c)). \end{aligned} \quad (4.13)$$

Then,

$$\int_0^{R_c} (as + b) (1 - \cos(2\pi ms)) ds \leq 0 \quad (4.14)$$

is satisfied for all $m \in \mathbb{N}$ if and only if $a \leq a_0$ with

$$a_0 := -b \max_{m \in \mathbb{N}} \frac{h(m)}{g(m)} \leq 0 \quad (4.15)$$

Proof. Note that the numerator of (4.11) is of the form $ag(m) + bh(m)$ for functions g and h , defined by (4.13). The condition (4.14) is equivalent to

$$a \leq -b \frac{h(m)}{g(m)} \quad \text{for all } m \in \mathbb{N}.$$

Herein, $h(m) \geq 0$ for all $m \geq 0$ since h is an increasing function. Further note that

$$\begin{aligned} g'(m) &= 2\pi (\pi m R_c^2 - R_c \sin(2\pi m R_c)) + 2\pi m (\pi R_c^2 - 2\pi R_c^2 \cos(2\pi m R_c)) + 2\pi R_c \sin(2\pi m R_c) \\ &= 4\pi^2 m R_c^2 (1 - \cos(2\pi m R_c)) \end{aligned}$$

is nonnegative implying that g is an increasing function with $g(0) = 0$. In particular, g and h are nonnegative functions for all $m \in \mathbb{N}$. Hence, (4.14) is satisfied for all $m \in \mathbb{N}$ if and only if $a < a_0$. Note that

$$\lim_{m \rightarrow \infty} \frac{h(m)}{g(m)} = \frac{2}{R_c}, \quad (4.16)$$

implying that

$$\sup_{m \in \mathbb{N}} \frac{h(m)}{g(m)} \in \mathbb{R}$$

by the nonnegativity and continuity of g and h .

For $R_c = 0.5$ we have

$$\frac{h(m)}{g(m)} = \begin{cases} \frac{2}{R_c}, & m \text{ even,} \\ \frac{4\pi^2 R_c}{2\pi^2 R_c^2 + \frac{2}{m^2}} < \frac{2}{R_c}, & m \text{ odd,} \end{cases}$$

implying that the maximum of $\frac{h(m)}{g(m)}$ over $m \in \mathbb{N}$ exists and

$$\max_{m \in \mathbb{N}} \frac{h(m)}{g(m)} = \frac{2}{R_c}$$

Hence, $a \leq a_0$ is equivalent to the necessary condition (4.12) for high-wave number stability for $R_c = 0.5$.

Let $R_c \in (0, 0.5)$ now. For $m > \frac{1}{\pi R_c}$, we have

$$\begin{aligned} \max_{m \in \mathbb{N}} \frac{h(m)}{g(m)} &\geq \frac{2\pi m (2\pi m R_c - \sin(2\pi m R_c))}{2\pi m (\pi m R_c^2 - R_c \sin(2\pi m R_c)) + 2} \\ &= \frac{2}{R_c} \left(1 + \frac{\pi m \sin(2\pi m R_c) - \frac{2}{R_c}}{2\pi m (\pi m R_c - \sin(2\pi m R_c)) + \frac{2}{R_c}} \right). \end{aligned}$$

Since $R_c \in (0, 0.5)$ there exists $m > \frac{1}{\pi R_c}$ such that $\pi m \sin(2\pi m R_c) - \frac{2}{R_c}$ and hence

$$\max_{m \in \mathbb{N}} \frac{h(m)}{g(m)} > \frac{2}{R_c}$$

in this case. □

Remark 4.4 From the proof of Lemma 4.3 it follows that

$$\frac{2}{R_c} \leq \max_{m \in \mathbb{N}} \frac{h(m)}{g(m)}. \quad (4.17)$$

The inequality in (4.17) is strict if and only if $R_c < 0.5$, i.e. (4.14) holds for $R_c < 0.5$ if and only if

$$a < -\frac{2b}{R_c}. \quad (4.18)$$

For $R_c = 0.5$, condition (4.14) is satisfied for any $a < 0$ satisfying the necessary condition (4.12) for high-wave number stability.

In Figure 2 we investigate the scaling factor of a_0 numerically, defined in (4.15). In Figure 2(A) the quotient h/g is shown as a function of $m \in \mathbb{N}$ for different values of the cutoff radius R_c . Note that the smaller R_c the larger the value of the maximum of h/g as shown in Figure 2(B). In Figures 2(C) and 2(D) we consider the quotient h/g scaled by R_c . Figure 2(C) shows that $R_ch/g \rightarrow 2$ as $m \rightarrow \infty$, independently of the value of R_c , and that the maximum of R_ch/g is obtained for smaller values of $m \in \mathbb{N}$ in general. The value of

$$R_c \max_{m \in \mathbb{N}} \frac{h(m)}{g(m)}$$

is shown in Figure 2(D) as a function of R_c . In particular, the scaled maximum is larger than 2 if and only if $R_c \in (0, 0.5)$ and is equal to 2 for $R_c = 0.5$. Hence, this numerical investigation is consistent with the results in Lemma 4.3.

Applying Lemma 4.3 to the specific form of the stability conditions for a single straight vertical line leads to the following stability results for the linear force coefficients (4.1):

Proposition 4.5 For $R_c \in (0, 0.5)$ the single straight vertical line is an unstable steady state of (1.3) for any $N \in \mathbb{N}$ sufficiently large and in the continuum limit $N \rightarrow \infty$ with forces of the form (2.9) for any linear coefficient functions f_s, f_l satisfying Assumption 4.1. For $R_c = 0.5$ the necessary stability conditions for a single straight vertical line are satisfied in the continuum limit $N \rightarrow \infty$ if

$$a_l \leq -\frac{2b_l}{R_c} \quad \text{and} \quad a_s = -\frac{b_s}{R_c} \quad (4.19)$$

holds in addition to the assumptions on the force coefficients f_s, f_l in Assumption 4.1.

Proof. Note that the real parts of the eigenvalues are of the form (4.9) with parameters (4.10). For stability we require $\Re(\lambda_k) \leq 0$ for $k = 1, 2$. Applying Lemma 4.3 together with Remark 4.4 for $R_c \in (0, 0.5)$ to the linear force coefficients (4.1) lead to the necessary stability conditions

$$a_l < -\frac{2b_l}{R_c} \quad \text{and} \quad a_s < -\frac{b_s}{R_c} \quad (4.20)$$

of the straight line with linear force coefficients. Purely repulsive forces along s are necessary for the occurrence of vertical line patterns. For f_s being purely repulsive as in Assumption 3.1, we require $a_s R_c + b_s \geq 0$ which clearly contradicts (4.20). Hence, the single straight vertical line is unstable for $R_c \in (0, 0.5)$ in the continuum limit $N \rightarrow \infty$ and for any $N \in \mathbb{N}$ sufficiently large.

For $R_c = 0.5$, Lemma 4.3 implies

$$a_l \leq -\frac{2b_l}{R_c} \quad \text{and} \quad a_s \leq -\frac{b_s}{R_c}$$

and together with the condition that f_s is purely repulsive we obtain (4.19). Note that the conditions (4.19) are consistent with each other since $a_l, a_s < 0$ and $b_l, b_s > 0$ by Assumption 4.1 and it is possible to choose the parameters a_l, a_s, b_l, b_s in such a way that both (4.19) and Assumption 4.1 are satisfied. \square

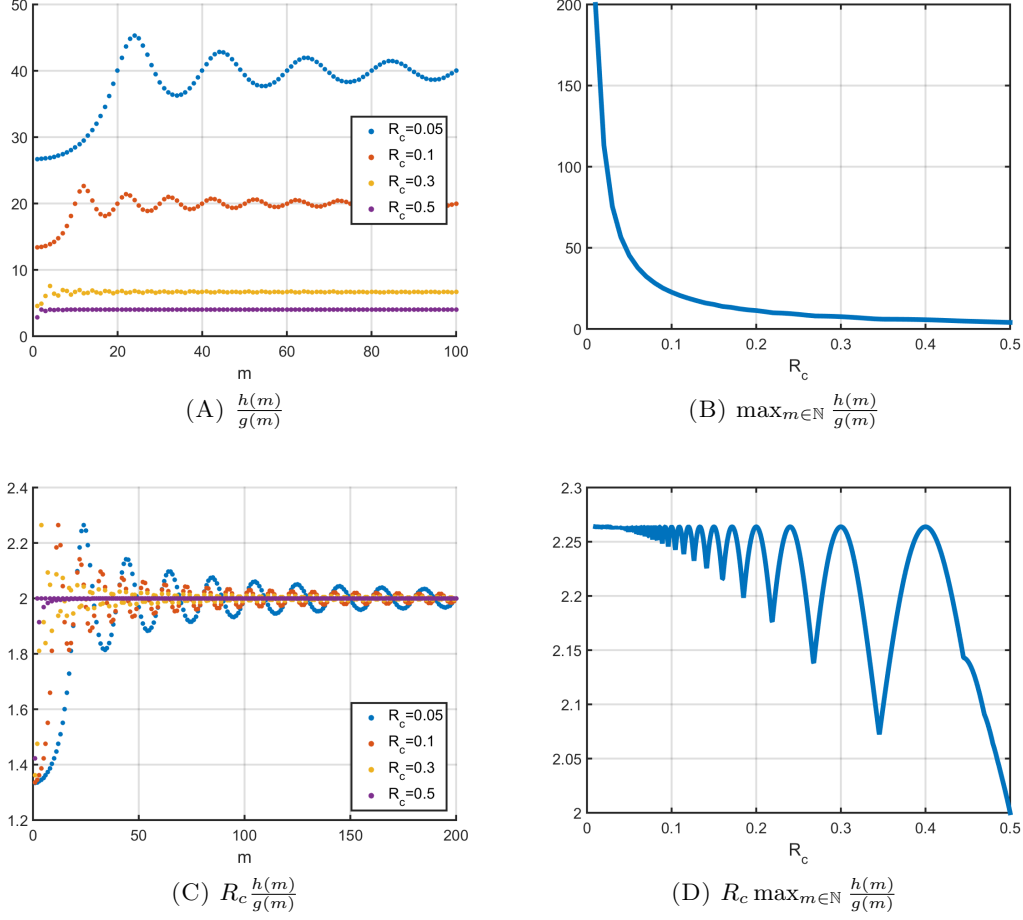


FIGURE 2. Scaling factor of a_0 in (4.15) as a functions of R_c where g, h are defined in (4.13)

Remark 4.6 In the linear case the necessary condition of stability of the straight vertical line can only be satisfied if $R_c = 0.5$ and condition (4.19) in Proposition 4.5 are satisfied. For the force coefficient f_l , the condition in (4.19) is equivalent to the high-wave number condition and hence high-wave number stability is the only necessary stability condition for the force coefficient f_l along l in the linear case. For the force coefficient f_s along s , Proposition 4.5 implies that the high-wave number stability condition is also the only necessary condition, provided f_s is purely repulsive as required in Assumption 3.1. Since the real part of the largest eigenvalue is zero, we cannot conclude stability/instability of the straight vertical line for $R_c = 0.5$ in the continuum limit $N \rightarrow \infty$ or any $N \in \mathbb{N}$ sufficiently large.

Since we have the relations $f_l = f_A + f_R$ and $f_s = \chi f_A + f_R$ between the force coefficients f_l, f_s in the general force formulation (2.7) and the repulsion and attractive forces in the Küken-Champod model (2.2) and (2.3) with force coefficients f_R and f_A , respectively, we have

$$a_l = a_A + a_R, \quad a_s = \chi a_A + a_R, \quad b_l = b_A + b_R, \quad b_s = \chi b_A + b_R.$$

Hence, Proposition 4.5 leads to a similar statement for the forces in the Küken-Champod model:

Corollary 4.7 For $R_c \in (0, 0.5)$ the single straight vertical line is an unstable steady state of (1.3) for any $N \in \mathbb{N}$ sufficiently large and for the continuum limit $N \rightarrow \infty$ with forces of the form (2.10) for any choice of parameters in the definition of the linear coefficient functions f_R, f_A in (4.2). For $R_c = 0.5$ the necessary stability conditions for the single straight vertical

line are satisfied in the continuum limit $N \rightarrow \infty$ if

$$a_A + a_R \leq -\frac{2(b_A + b_R)}{R_c} \quad \text{and} \quad \chi a_A + a_R = -\frac{\chi b_A + b_R}{R_c} \quad (4.21)$$

holds in addition to the assumptions on a_A, a_R, b_A, b_R in Remark 4.2. This does not guarantee the stability/instability of the straight vertical line for $R_c = 0.5$ for $N \in \mathbb{N}$ sufficiently large and for the continuum limit $N \rightarrow \infty$.

4.2. Algebraically decaying force coefficients. Since the straight vertical line is unstable for $N \in \mathbb{N}$ sufficiently large and for $N \rightarrow \infty$ for the linear force coefficient f_s along s for $R_c \in (0, 0.5)$ we consider faster decaying force coefficients f_s in the sequel. In this section we consider

$$\frac{c}{(1 + a|d|)^b}$$

for $a > 0$, $b > 0$ and $c > 0$. To satisfy the necessary condition $f_s(R_c) = 0$ for f_s in (3.17) for high-wave number stability of a straight vertical line, we consider

$$f_s(|d|) = \frac{c}{(1 + a|d|)^b} - \frac{c}{(1 + aR_c)^b}.$$

To guarantee that the term $a|d|$ for $|d| \in [0, R_c]$ dominates the denominator and to avoid too large jumps we require $a \gg 1$ additionally. Without loss of generality we can assume that $c = 1$ since this positive multiplicative constant leads to a rescaled stability condition but is not relevant for change of sign of the eigenvalues. Hence, we consider the algebraically decaying force coefficient

$$f_s(|d|) = \frac{1}{(1 + a|d|)^b} - \frac{1}{(1 + aR_c)^b} \quad (4.22)$$

in the sequel.

Proposition 4.8 *For the single straight vertical line to be a stable steady state of (1.3) with forces of the form (2.1) for any $n \in \mathbb{N}$ sufficiently large and for the continuum limit $N \rightarrow \infty$ with algebraically decaying force coefficients f_s of the form (4.22) it is necessary that*

$$b > 1 \quad \text{and} \quad \frac{2}{a(b-1)} < R_c.$$

Proof. Because of the definition of the eigenvalues (3.13) we consider

$$\begin{aligned} & \int_0^{R_c} (f_s(s) + f'_s(s)s) (1 - \cos(-2\pi ms)) ds \\ &= \int_0^{R_c} \frac{1}{(1 + as)^{b+1}} (1 + as(1 - b)) (1 - \cos(-2\pi ms)) ds \\ & \quad - \frac{1}{(1 + aR_c)^b} \left(R_c + \frac{1}{2\pi m} \sin(-2\pi mR_c) \right). \end{aligned} \quad (4.23)$$

The linear function $1 + as(1 - b)$ is positive for $s \in (0, s_0)$ and negative for $s \in (s_0, R_c)$ where

$$s_0 = \frac{1}{a(b-1)} \in (0, R_c)$$

implying $b > 1$. Note that the integral on the right-hand side of (4.23) can be rewritten as

$$\int_0^{R_c} g(s) ds = \int_0^{s_0} g(s) ds + \int_{s_0}^{R_c} g(s) ds$$

where

$$g(s) = \frac{1}{(1+as)^{b+1}} (1+as(1-b)) (1-\cos(-2\pi ms))$$

is nonnegative on $[0, s_0]$ and not positive on $[s_0, R_c]$ by the definition of s_0 and the fact that $1 - \cos(-2\pi ms) \in (0, 2)$. Setting

$$h(s) = \frac{1}{(1+as)^{b+1}}$$

note that $h(R_c) < h(s_0) < h(0) = 1$. A lower bound of the integral can be obtained by estimating $h(s)$ on $[0, s_0]$ by $h(s_0)$ due to the nonnegativity of the integrand and since the integrand changes sign at s_0 the factor $h(s)$ can be replaced by its maximum on $[s_0, R_c]$, i.e. by $h(s_0)$, for obtaining a lower bound of the integral. Hence, a lower bound of the integral is given by

$$\begin{aligned} & \frac{1}{(1+as_0)^{b+1}} \int_0^{R_c} (1+as(1-b)) (1-\cos(-2\pi ms)) ds \\ & - \frac{1}{(1+aR_c)^b} \left(R_c + \frac{1}{2\pi m} \sin(-2\pi mR_c) \right) \\ & = \frac{1}{(1+as_0)^{b+1}} \left(\frac{2\pi m (\pi m R_c (pR_c + 2q) - (pR_c + q) \sin(2\pi mR_c)) - p \cos(2\pi mR_c) + p}{4\pi^2 m^2} \right) \\ & - \frac{1}{(1+aR_c)^b} \left(R_c + \frac{1}{2\pi m} \sin(-2\pi mR_c) \right) \end{aligned}$$

with $p = a(1-b)$ and $q = 1$ where the explicit computation results from the discussion of the linear force coefficients in (4.11). For large values of m the first term dominates and we require

$$pR_c + 2q = a(1-b)R_c + 2 < 0.$$

This concludes the proof. \square

In the sequel, we can restrict ourselves to algebraically decaying force coefficients (4.22) with $a > 0$, $b > 1$ due to Proposition 4.8. We show that the straight vertical line (3.3) is an unstable steady state for any $N \in \mathbb{N}$ sufficiently large and in the continuum limit $N \rightarrow \infty$ in this case. Due to the definition of the eigenvalues in (3.13) in Theorem 3.3 it is sufficient to show that there exists $m \in \mathbb{N}$ such that

$$0 < \int_0^{R_c} (f_s(s) + f'_s(s)s) (1-\cos(-2\pi ms)) ds.$$

This is equivalent to showing that there exists $m \in \mathbb{N}$ such that

$$\begin{aligned} 0 < \int_0^{R_c} \frac{1}{(1+as)^{b+1}} (1+as(1-b)) (1-\cos(-2\pi ms)) ds \\ - \frac{1}{(1+aR_c)^b} \left(R_c + \frac{1}{2\pi m} \sin(-2\pi mR_c) \right). \end{aligned} \tag{4.24}$$

is satisfied.

Lemma 4.9 *For any $a > 0$, $b > 1$ and $R_c \in (0, 0.5]$ there exists $m \in \mathbb{N}$ such that (4.24) is satisfied.*

Proof. We denote the incomplete Gamma function by

$$\Gamma(y, z) = \int_z^\infty s^{y-1} \exp(-s) ds.$$

Then the right-hand side of (4.24) can be written as

$$\begin{aligned} & -\frac{1}{4a\pi m(1+aR_c)^b} \left(2a \sin(-2\pi m R_c) \right. \\ & + \Re \left[\sin\left(\frac{2\pi m}{a}\right) m^{b+1} \left(c_1 \Gamma\left(-b, \frac{2i\pi m}{a}\right) + c_2 \Gamma\left(-b, \frac{2i\pi(1+aR_c)m}{a}\right) \right) \right. \\ & + \sin\left(\frac{2\pi m}{a}\right) m^b \left(c_3 \Gamma\left(1-b, \frac{2i\pi m}{a}\right) + c_4 \Gamma\left(1-b, \frac{2i\pi(1+aR_c)m}{a}\right) \right) \\ & + \cos\left(\frac{2\pi m}{a}\right) m^{b+1} \left(c_5 \Gamma\left(-b, \frac{2i\pi m}{a}\right) + c_6 \Gamma\left(-b, \frac{2i\pi(1+aR_c)m}{a}\right) \right) \\ & \left. \left. + \cos\left(\frac{2\pi m}{a}\right) m^b \left(c_7 \Gamma\left(1-b, \frac{2i\pi m}{a}\right) + c_8 \Gamma\left(1-b, \frac{2i\pi(1+aR_c)m}{a}\right) \right) \right] \right) \end{aligned}$$

for constants $c_i \in \mathbb{C}, i = 1, \dots, 8$, depending on a, b and R_c , but independent of m where not all constants c_i are equal to zero. Note that

$$|\Gamma(-y, izm)| = \left| \int_{izm}^{\infty} s^{-y-1} \exp(-s) ds \right| \leq (zm)^{-y-1}$$

for $y, z \in \mathbb{R}, y > 0$, implying that the right-hand side of (4.24) is of the form

$$-\frac{1}{4a\pi m(1+aR_c)^b} \left(2a \sin(-2\pi m R_c) + \bar{c}_1 \sin\left(\frac{2\pi m}{a}\right) + \bar{c}_2 \cos\left(\frac{2\pi m}{a}\right) \right)$$

for constants $\bar{c}_1, \bar{c}_2 \in \mathbb{R}$, independent of m . Hence, we have oscillations around zero for all $R_c \in (0, 0.5]$. In particular, this implies that there exists an $m \in \mathbb{N}$ such that (4.24) is satisfied. \square

Corollary 4.10 *For any cutoff radius $R_c \in (0, 0.5]$ the single straight vertical line is an unstable steady state of (1.3) for any $N \in \mathbb{N}$ sufficiently large and for the continuum limit $N \rightarrow \infty$ with forces of the form (2.1) with algebraically decaying force coefficients f_s of the form (4.22) with $b > 0$.*

4.3. Exponential force coefficients. In this section we consider exponentially decaying force coefficient f_s along s and short-range repulsive, long-range attractive forces along l such that the necessary condition (3.17) for high-wave number stability is satisfied.

To express the force coefficient along l in terms of exponentially decaying functions we consider

$$f_l: \mathbb{R}_+ \rightarrow \mathbb{R}, \quad f_l(|d|) = c_{l_1} \exp(-e_{l_1}|d|) + c_{l_2} \exp(-e_{l_2}|d|) \quad (4.25)$$

for parameters $c_{l_1}, c_{l_2}, e_{l_1}$ and e_{l_2} with $e_{l_1} > 0$ and $e_{l_2} > 0$. Note that exponentially decaying functions are either purely repulsive or purely attractive, depending on the sign of the multiplicative parameter. Since we require f_l to be short-range repulsive, long-range attractive we consider the sum of two exponentially decaying functions here. Without loss of generality we assume that the first summand in (4.25) is repulsive and the second one is attractive, i.e. $c_{l_1} > 0 > c_{l_2}$. To guarantee that f_l is short-range repulsive we require $c_{l_1} > |c_{l_2}|$. For long-range attractive forces we require that the second term decays slower, i.e. $e_{l_1} > e_{l_2}$. These assumptions lead to the parameter choice:

$$c_{l_1} > 0 > c_{l_2}, \quad c_{l_1} > |c_{l_2}| \quad \text{and} \quad e_{l_1} > e_{l_2} > 0. \quad (4.26)$$

Note that we have for constants $c, e_l \in \mathbb{R}$:

$$\int_0^{R_c} c \exp(-e_l s) ds = (1 - \exp(-e_l R_c)) \frac{c}{e_l}.$$

Hence, we require

$$(1 - \exp(-e_{l_1} R_c)) \frac{c_{l_1}}{e_{l_1}} + (1 - \exp(-e_{l_2} R_c)) \frac{c_{l_2}}{e_{l_2}} \leq 0$$

as in the necessary condition for high-wave number stability, implying

$$\frac{c_{l_1}}{e_{l_1}} \leq \frac{|c_{l_2}|}{e_{l_2}}.$$

Since

$$\begin{aligned} \int_0^{R_c} c_{l_1} \exp(-e_{l_1} s) (1 - \cos(-2\pi m s)) ds &> 0, \\ \int_0^{R_c} c_{l_2} \exp(-e_{l_2} s) (1 - \cos(-2\pi m s)) ds &< 0, \end{aligned}$$

for all $m \in \mathbb{N}$ the parameters $c_{l_1}, c_{l_2}, e_{l_1}, e_{l_2}$ in (4.26) can clearly be chosen in such a way that

$$\int_0^{R_c} f_l(s) (1 - \cos(-2\pi m s)) ds \leq 0 \quad (4.27)$$

for all $m \in \mathbb{N}$ for f_l in (4.25) with a cutoff radius $R_c \in (0, 0.5]$.

For the purely repulsive force coefficient f_s we consider a function of the form

$$f_s: \mathbb{R}_+ \rightarrow \mathbb{R}, \quad f_s(|d|) = c \exp(-e_s |d|) - c \exp(-e_s R_c) \quad (4.28)$$

with $c > 0$ and $e_s > 0$. The first term in (4.28) represents the exponential decay of the force coefficient. To satisfy the high-wave number stability condition, we require $f_s(R_c) = 0$ as in (3.17). This can be modelled by assuming that $e_s \gg 1$ so that $\exp(-e_s R_c)$ is a small positive number. Alternatively, subtracting the constant $c \exp(-e_s R_c)$ as in (4.28) leads to $f_s(R_c) = 0$ and this additional constant only changes the force coefficient f_s slightly.

Thus, we make the following assumption in the sequel:

Assumption 4.11 *We assume that the purely repulsive, exponentially decaying force coefficient f_s along s is given by*

$$f_s(|d|) = c \exp(-e_s |d|) - c \exp(-e_s R_c)$$

in (4.28) where $c > 0$ and $e_s \gg 1$. For the forces along l we either consider linear or exponentially decaying force coefficients. For a linear force coefficient

$$f_l(|d|) = a_l |d| + b_l,$$

we assume that the parameters a_l, b_l satisfy the sign conditions $a_l < 0, b_l > 0$ in Assumption 4.1 as well as the necessary stability condition along l in (4.19). For an exponentially decaying force coefficient f_l we assume that f_l is of the form

$$f_l(|d|) = c_{l_1} \exp(-e_{l_1} |d|) + c_{l_2} \exp(-e_{l_2} |d|)$$

for parameters

$$c_{l_1} > 0 > c_{l_2}, \quad c_{l_1} > |c_{l_2}| \quad \text{and} \quad e_{l_1} > e_{l_2} > 0$$

as in (4.25)–(4.26) such that the necessary stability condition (4.27) for a straight vertical line is satisfied for all $m \in \mathbb{N}$.

Theorem 4.12 *The straight vertical line is stable for the particle model (1.3) for any $N \in \mathbb{N}$ sufficiently large with exponentially decaying force coefficient*

$$f_s(|d|) = c \exp(-e_s |d|) - c \exp(-e_s R_c)$$

with $e_s > 0$ and linear or exponentially decaying force coefficient f_l as in Assumption 4.11 for a cutoff radius $R_c = 0.5$. For $R_c \in (0, 0.5)$ the straight vertical line is an unstable steady state to (1.3) for any $N \in \mathbb{N}$ sufficiently large and for the continuum limit $N \rightarrow \infty$ for any exponential decay $e_s > 0$.

Proof. Due to the assumptions on f_l in Assumption 4.11 the real part for the first eigenvalue in (3.13), given by

$$\Re(\lambda_1(m)) = 2 \int_0^{R_c} f_l(s) (1 - \cos(-2\pi ms)) ds,$$

is not positive for any $m \in \mathbb{N}$. For the non-positivity of the real part of the second eigenvalue in (3.13), given by

$$\Re(\lambda_2(m)) = 2 \int_0^{R_c} (f_s(s) + f'_s(s)s) (1 - \cos(-2\pi ms)) ds,$$

it is sufficient to require

$$\int_0^{R_c} (f_s(s) + s f'_s(s)) (1 - \cos(2\pi ms)) ds \leq 0, \quad (4.29)$$

where the left-hand side is given by

$$\begin{aligned} & c \int_0^{R_c} (\exp(-e_s s)(1 - e_s s) - \exp(-e_s R_c)) (1 - \cos(2\pi ms)) ds \\ &= -\frac{ce_s \exp(-e_s R_c)}{2\pi m (e_s^2 + 4\pi^2 m^2)^2} [2\pi m (e_s^3 R_c + 4\pi^2 m^2 (e_s R_c - 2)) \cos(2\pi m R_c) \\ & \quad - (e_s^3 + 4\pi^2 e_s^2 m^2 R_c + 12\pi^2 e_s m^2 + 16\pi^4 m^4 R_c) \sin(2\pi m R_c) + 16\pi^3 m^3 \exp(e_s R_c)]. \end{aligned} \quad (4.30)$$

For $R_c = 0.5$ we have $\sin(2\pi m R_c) = 0$ and the right-hand side of (4.30) simplifies to $g(m)h(m)$ where

$$\begin{aligned} g(m) &= -\frac{ce_s \exp(-e_s R_c)}{(e_s^2 + 4\pi^2 m^2)^2}, \\ h(m) &= (e_s^3 R_c + 4\pi^2 m^2 (e_s R_c - 2)) \cos(2\pi m R_c) + 8\pi^2 m^2 \exp(e_s R_c). \end{aligned}$$

For determining the limit $m \rightarrow \infty$ of $g(m)h(m)$ note that the leading order term of g is m^{-4} while the highest order term of h is m^2 , implying that the product $g(m)h(m)$, i.e. the right-hand side of (4.30), goes to zero as $m \rightarrow \infty$.

Note that for $R_c = 0.5$ we have

$$\cos(2\pi m R_c) = \begin{cases} 1, & m \text{ even}, \\ -1, & m \text{ odd}. \end{cases}$$

Let us consider $e_s > 0$ with $e_s \leq 4$ first, i.e. $e_s R_c \leq 2$. Then,

$$h(m) = \begin{cases} e_s^3 R_c + 4\pi^2 m^2 (e_s R_c - 2 + 2 \exp(e_s R_c)), & m \text{ even}, \\ -e_s^3 R_c + 4\pi^2 m^2 (-e_s R_c + 2 + 2 \exp(e_s R_c)), & m \text{ odd}. \end{cases}$$

Note that $g(m) < 0$ for all $m \in \mathbb{N}$ and $h(m) > 0$ for all even m since $2 \exp(e_s R_c) > 2$. For m odd, note that the term in brackets is positive and a lower bound of h is given by

$$-16e_s R_c + 4\pi^2 (-e_s R_c + 2 + 2 \exp(e_s R_c)) \geq 8\pi^2 (-e_s R_c + 1 + \exp(e_s R_c)),$$

which is clearly positive. Hence $h(m)$ is positive for all $m \in \mathbb{N}$ and thus $g(m)h(m) < 0$, provided $e_s \leq 4$ and $R_c = 0.5$, implying that (4.29) is satisfied for all $m \in \mathbb{N}$ in this case.

Let us now consider $e_s R_c > 2$. Note that a lower bound of h is obtained for $\cos(2\pi m R_c) = -1$, leading to the upper bound

$$g(m) [- (e_s^3 R_c + 4\pi^2 m^2 (e_s R_c - 2)) + 8\pi^2 m^2 \exp(e_s R_c)]$$

of $g(m)h(m)$ since $g(m) < 0$. This upper bound can be rewritten as

$$g(m) [-e_s^3 R_c + 4\pi^2 m^2 (-e_s R_c + 2 + 2 \exp(e_s R_c))].$$

Note that $-e_s R_c + 2 + 2 \exp(e_s R_c) > 0$. Besides,

$$\frac{e_s^3 R_c}{4\pi^2 (-e_s R_c + 2 + 2 \exp(e_s R_c))} < 1$$

is satisfied for all $e_s > 4$, implying

$$-e_s^3 R_c + 4\pi^2 m^2 (-e_s R_c + 2 + 2 \exp(e_s R_c)) > 0$$

for all $m \in \mathbb{N}$. Hence, the right-hand side of (4.30) is negative for all $m \in \mathbb{N}$. In particular, this shows that condition (4.29) is satisfied for all $m \in \mathbb{N}$ for $R_c = 0.5$.

For $R_c \in (0, 0.5)$ we have $\sin(2\pi m R_c) > 0$ for countably many $m \in \mathbb{N}$. In particular, there exists $\delta > 0$ and a countably infinite set $\mathcal{N} \subset \mathbb{N}$ such that $\sin(2\pi m R_c) > \delta$ for all $m \in \mathcal{N}$. Hence the second term in (4.30) is negative with upper bound

$$-(e_s^3 + 4\pi^2 e_s^2 m^2 R_c + 12\pi^2 e_s m^2 + 16\pi^4 m^4 R_c) \delta < 0$$

for all $m \in \mathcal{N}$. This implies that the right-hand side of (4.30) can be estimated from below by

$$\begin{aligned} & \frac{g(m)}{2\pi m} [2\pi m \max\{e_s^3 R_c + 4\pi^2 m^2 (e_s R_c - 2), -e_s^3 R_c - 4\pi^2 m^2 (e_s R_c - 2)\} \\ & + 16\pi^3 m^3 \exp(e_s R_c) - (e_s^3 + 4\pi^2 e_s^2 m^2 R_c + 12\pi^2 e_s m^2 + 16\pi^4 m^4 R_c) \delta] \end{aligned}$$

for all $m \in \mathcal{N}$ since $g(m) < 0$ for all $m \in \mathbb{N}$. Thus, there exists $m_0 \in \mathcal{N}$ such that the term in square brackets is negative for all $m \in \mathcal{N}$ with $m \geq m_0$ since the highest order term of power m^4 in the square brackets dominates for m large enough. In particular, $g(m_0) < 0$ implies that we have found a positive lower bound of the right-hand side in (4.30) and hence, stability cannot be achieved in the case $R_c \in (0, 0.5)$, both for $N \in \mathbb{N}$ sufficiently large and in the continuum limit $N \rightarrow \infty$. \square

Remark 4.13 For $R_c \in (0, 0.5)$ no stability can be shown analytically. However, note that an upper bound of the integral

$$\int_0^{R_c} (f_s(s) + s f'_s(s)) (1 - \cos(2\pi m s)) ds \quad (4.31)$$

in the necessary stability condition (4.29) is given by

$$\begin{aligned} & -\frac{ce_s \exp(-e_s R_c)}{2\pi m (e_s^2 + 4\pi^2 m^2)^2} [-2\pi m (e_s^3 R_c + 4\pi^2 m^2 (e_s R_c - 2)) \\ & - (e_s^3 + 4\pi^2 e_s^2 m^2 R_c + 12\pi^2 e_s m^2 + 16\pi^4 m^4 R_c) + 16\pi^3 m^3 \exp(e_s R_c)] \\ & = -\frac{ce_s \exp(-e_s R_c)}{2\pi m (e_s^2 + 4\pi^2 m^2)^2} [-e_s^3 - 2\pi e_s^3 R_c m - (4\pi^2 e_s^2 R_c + 12\pi^2 e_s) m^2 \\ & + (-8\pi^3 (e_s R_c - 2) + 16\pi^3 \exp(e_s R_c)) m^3 - 16\pi^4 R_c m^4]. \end{aligned} \quad (4.32)$$

due to (4.30). For $\exp(e_s R_c) \gg 1$ there exists $m_0 \in \mathbb{N}$ of order $\exp(e_s R_c) \gg 1$ such that the term $16\pi^3 m^3 \exp(e_s R_c)$ is the dominating term in the upper bound (4.32) of the integral (4.31) for all $m \in \mathbb{N}$ with $m \leq m_0$. Hence negativity of the upper bound (4.32) and thus of the integral (4.31) in the necessary stability condition can be guaranteed for all $m \leq m_0$. For $m > m_0$, however, the highest order term of power m^4 dominates the sum. Since $m_0 \gg 1$, we have stability for $N \in \mathbb{N}$ sufficiently large and for the continuum limit $N \rightarrow \infty$ for almost all, but finitely many, Fourier modes for $R_c \in (0, 0.5)$ and $e_s \gg 1$.

The integral (4.31) is explicitly evaluated in (4.30). For large values of $m \in \mathbb{N}$ the highest order term in (4.30) is associated with the summand $16\pi^4 m^4 R_c \sin(2\pi m R_c)$ and can be written in the form

$$\frac{8\pi^3 e_s \exp(-e_s R_c) R_c m^3 \sin(2\pi m R_c)}{(e_s^2 + 4\pi^2 m^2)^2}.$$

Here, the numerator increases as m^3 for large m while the denominator is of order m^4 , multiplied by a factor $\exp(-e_s R_c) \ll 1$, leading to decaying sinusoidal oscillations around zero as m increases. Since this approximation is only valid for $m > m_0 \gg 1$ the absolute value of the right-hand side in (4.30) may be so small that it is numerically zero and one may see stable vertical line patterns for exponentially decaying force coefficients f_s along s for $R_c \in (0, 0.5)$ for $N \in \mathbb{N}$ sufficiently large, see the numerical experiment in Figure 5(E).

Corollary 4.14 *Let $c_1, c_2 \in \mathbb{R}$ with $c_1 > 0$, $c_1 > |c_2|$ be given. There exist parameters $e_2 \geq e_1 > 0$ such that the straight vertical line is stable for the particle model (1.3) for $N \in \mathbb{N}$ sufficiently large for the exponentially decaying force coefficient f_s along s given by*

$$f_s: \mathbb{R}_+ \rightarrow \mathbb{R}, \quad f_s(|d|) = c_1 \exp(-e_1 |d|) + c_2 \exp(-e_2 |d|) - c \quad (4.33)$$

with

$$c = c_1 \exp(-e_1 R_c) + c_2 \exp(-e_2 R_c)$$

and a linear or an exponential force coefficient f_l along l as in Assumption 4.11 for a cutoff radius $R_c = 0.5$. For the continuum limit $N \rightarrow \infty$ stability/instability cannot be concluded.

Proof. For the stability of the straight vertical line for $N \in \mathbb{N}$ sufficiently large we require that the force coefficient f_s in (4.33) is purely repulsive and hence at least one of the constants c_1, c_2 has to be positive. Since we can assume $c_1 > 0$ without loss of generality this implies that c_1 is a repulsive multiplicative factor, while the sign of c_2 is not given by the assumptions. Hence, we require that the first term in the definition of f_s in (4.33) decays slower than the second one, implying $0 < e_1 \leq e_2$. Hence, the conditions on the parameters are verified.

As in the proof of Theorem 4.12 we evaluate integrals of the form (4.30) where the term with factor $\sin(2\pi m R_c)$ vanishes for our choice of $R_c = 0$. If $c_2 \geq 0$ one can choose e_1, e_2 sufficiently large such that the term $16\pi^3 m^3 \exp(e_k R_c)$, $k = 1, 2$, in the square brackets in (4.30) dominates as in the proof of Theorem 4.12, leading to the stability of the vertical straight line for $N \in \mathbb{N}$ sufficiently large. For $c_2 < 0$ one can choose e_1, e_2 sufficiently large such that the term $16\pi^3 m^3 \exp(e_k R_c)$, $k = 1, 2$, dominate the square brackets. However, since $c_1 > 0 > c_2$ we require in addition that the term with multiplicative factor c_1 dominates over the term with multiplicative factor c_2 , leading to the condition

$$\begin{aligned} & -\frac{c_1 e_1 \exp(-e_1 R_c)}{2\pi m (e_1^2 + 4\pi^2 m^2)^2} [16\pi^3 m^3 \exp(e_1 R_c)] + \frac{|c_2| e_2 \exp(-e_2 R_c)}{2\pi m (e_2^2 + 4\pi^2 m^2)^2} [16\pi^3 m^3 \exp(e_2 R_c)] \\ & = -\frac{16\pi^3 m^3 c_1 e_1}{2\pi m (e_1^2 + 4\pi^2 m^2)^2} + \frac{16\pi^3 m^3 |c_2| e_2}{2\pi m (e_2^2 + 4\pi^2 m^2)^2} < 0 \end{aligned}$$

which is equivalent to

$$-c_1 e_1 (e_2^2 + 4\pi^2 m^2)^2 + |c_2| e_2 (e_1^2 + 4\pi^2 m^2)^2 < 0.$$

Since $c_1 > |c_2|$ and $e_2 \geq e_1 > 0$ by assumption this condition is satisfied for $e_2 > e_1$ sufficiently large. Hence, stability of the straight vertical line can be achieved for $N \in \mathbb{N}$ sufficiently large. \square

The force coefficient f_s of the form (4.33) along s is motivated by the force coefficients in the Kücken-Champod model. Here, $f_s = \chi f_A + f_R$ is considered for $\chi \in [0, 1]$. This corresponds to the sum of an attractive and a repulsive force coefficient as in (4.33) for $c_1 > 0 > c_2$ where the repulsive term, i.e. $c_1 > |c_2|$ dominates. This motivates that we obtain stability of the straight vertical line for the force coefficients in the Kücken-Champod model for $N \in \mathbb{N}$ sufficiently large if an additional constant is considered in the definition of f_s .

4.4. Kücken-Champod model. For the specific forces in the Kücken-Champod model, given by the repulsive and attractive force coefficients f_R and f_A in (2.4) and (2.5), respectively, we require the non-positivity of the real parts of the eigenvalues $\lambda_k, k = 1, 2$, given by

$$\begin{aligned}\Re(\lambda_1(m)) &= 2 \int_0^{R_c} f_l(s) (1 - \cos(-2\pi ms)) ds, \\ \Re(\lambda_2(m)) &= 2 \int_0^{R_c} (f_s(s) + f'_s(s)s) (1 - \cos(-2\pi ms)) ds\end{aligned}$$

in (3.13) where $f_l = f_A + f_R$ and $f_s = \chi f_A + f_R$. In Figure 3 we evaluate $\Re(\lambda_k)$ numerically for the force coefficients (2.4) and (2.5) in the Kücken-Champod model for the parameters in (2.6) and a cutoff radius $R_c = 0.5$. Clearly, $\Re(\lambda_1) \leq 0$, while $\Re(\lambda_2)$ is negative for small modes m but tends to zero for large modes m . Investigating the high-wave number stability for the forces

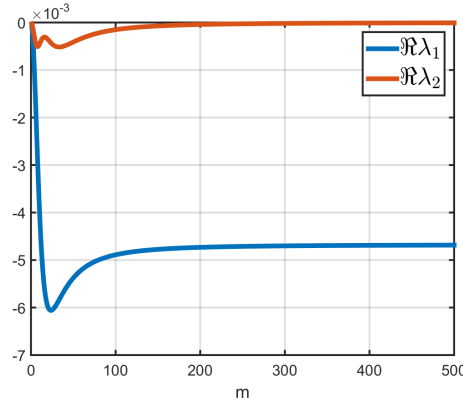


FIGURE 3. $\Re(\lambda_i)$ in (3.13) as a function of m for the force coefficients f_R in (2.4) and f_A in (2.5) of repulsion force (2.2) and attraction force (2.3), respectively, for parameter values in (2.6) where $f_l = f_A + f_R$ and $f_s = \chi f_A + f_R$

in the Kücken-Champod model can be done analytically. For the general necessary high-wave number condition (3.17) for λ_1 we require

$$\int_0^{R_c} f_l ds \leq 0.$$

Note that

$$\begin{aligned}& \int_0^{R_c} \exp(-e_R s) (\alpha s^2 + \beta) - \gamma \exp(-e_A s) s ds \\ &= \frac{\alpha (\exp(-e_R R_c) (-e_R R_c (e_R R_c + 2) - 2) + 2)}{(e_R)^3} + \frac{\beta - \beta \exp(-e_R R_c)}{e_R} \\ & \quad - \frac{\gamma (1 - \exp(-e_A R_c) (e_A R_c + 1))}{(e_A)^2} \\ &\approx \frac{2\alpha}{(e_R)^3} + \frac{\beta}{e_R} - \frac{\gamma}{(e_A)^2}\end{aligned}$$

which is clearly negative for the choice of parameters in (2.6). For the high-wave stability we also consider the condition associated with λ_2 , leading to the condition

$$\int_0^{R_c} f_s(s) + f'_s(s)s \leq 0.$$

Evaluating this integral gives

$$\begin{aligned}
& \int_0^{R_c} \exp(-e_R s) (\alpha (3s^2 - e_R s^3) + \beta (1 - e_R s)) - \chi \gamma \exp(-e_A s) s (2 - e_A s) \, ds \\
&= R_c (R_c (\alpha R_c \exp(-e_R R_c) - \chi \gamma \exp(-e_A R_c)) + \beta \exp(-e_R R_c)) \\
&= R_c (f_R(R_c) + \chi f_A(R_c))
\end{aligned}$$

for f_R and f_A defined in (2.4) and (2.5), respectively. Note that

$$\chi f_A(R_c) + f_R(R_c) = 4.8144 \cdot 10^{-21},$$

implying that the straight vertical line is high-wave number unstable for any $N \in \mathbb{N}$ sufficiently large and for the continuum limit $N \rightarrow \infty$ for the Kücken-Champod model with force coefficients f_R and f_A in (2.4) and (2.5), respectively, and the parameters in (2.6) since $f_s(R_c) = 0$ is necessary for the high-wave number stability of the straight vertical line, compare Proposition 3.5. Hence, the straight vertical line is unstable for any $N \in \mathbb{N}$ sufficiently large and in the continuum limit $N \rightarrow \infty$. However,

$$\chi f_A(R_c) + f_R(R_c)$$

is very small so that it is numerically zero and thus this instability may not be observed in numerical simulations.

Since $\chi f_A(R_c) + f_R(R_c) = 4.8144 \cdot 10^{-21}$ subtracting the constant $\chi f_A(R_c) + f_R(R_c)$, as suggested in Section 4.3 for the exponentially decaying force coefficient f_s along s , only changes the force coefficient slightly. Hence, we consider

$$f_s(|d|) = \chi f_A(|d|) + f_R(|d|) - (\chi f_A(R_c) + f_R(R_c)). \quad (4.34)$$

This leads to $f_s(R_c) = 0$, i.e. the high-wave number stability of the vertical straight line is achieved.

Note that it is not possible to analyse the stability of the straight vertical line for all modes $m \in \mathbb{N}$ for the forces f_R and f_A in (2.4) and (2.5) in the Kücken-Champod model analytically for all possible parameter values due to the large number of parameters in the model and the form of the force coefficients strongly depends on the choice of parameters. In Corollary 4.14, however, we investigated the stability of the straight vertical line for $N \in \mathbb{N}$ sufficiently large where f_s is the sum of the positive term $c_1 \exp(-e_1 |d|)$, the negative term $c_2 \exp(-e_2 |d|)$ and a constant to guarantee $f_s(R_c) = 0$ where $c_1 > |c_2| > 0$. Besides, we required $e_1 < e_2$ for the positivity of the sum $c_1 \exp(-e_1 |d|) + c_2 \exp(-e_2 |d|)$ and showed stability of the straight vertical line for $N \in \mathbb{N}$ sufficiently large provided the parameters $e_1, e_2 > 0$ are chosen sufficiently large enough. In Figure 1 the absolute value of the terms χf_A and f_R in the definition of f_s in (4.34) for the Kücken-Champod model are plotted for the parameters in (2.6). As in Corollary 4.14 the positive term always dominates and the terms χf_A and f_R have fast exponential decays. This suggests that the straight vertical line is a stable steady state for the Kücken-Champod model for $N \in \mathbb{N}$ sufficiently large with revised force coefficient f_s in (4.34). Besides, the numerical evaluation of the real part of the eigenvalue λ_2 for f_s in (4.34) instead of $f_s = \chi f_A + f_R$, i.e. with the additional constant $-(\chi f_A(R_c) + f_R(R_c))$ leads to non-positivity of the real part of the eigenvalue λ_2 .

4.5. Summary. In this section, we summarize the results from the previous subsections on the stability of the straight vertical line (3.3) of the particle model (1.3) with linear, algebraically decaying and exponentially decaying force coefficients for different values of the cutoff radius $R_c \in (0, 0.5]$. This summary is shown in Table 1.

TABLE 1. Stability/Instability of the straight vertical line (3.3) for the particle model (1.3) with force coefficients f_s along s and different cutoff radii $R_c \in (0, 0.5]$.

Force coefficient f_s along s	$R_c \in (0, 0.5)$	$R_c = 0.5$
Linear force coefficient (4.1)	Instability for any $N \in \mathbb{N}$ sufficiently large and for $N \rightarrow \infty$ (see Theorem 4.5)	Stability or instability since stability conditions are satisfied with equality (see Corollary 4.5)
Algebraically decaying force coefficient (4.22)	Instability for any $N \in \mathbb{N}$ sufficiently large and for $N \rightarrow \infty$ (see Corollary 4.10)	Instability for any $N \in \mathbb{N}$ sufficiently large and for $N \rightarrow \infty$ (see Corollary 4.10)
Exponentially decaying force coefficient (4.28)	Instability for any $N \in \mathbb{N}$ sufficiently large and for $N \in \mathbb{N}$ (see Theorem 4.12), but stability may be seen in numerical simulations (see Remark 4.13)	Stability for any $N \in \mathbb{N}$ sufficiently large (see Theorem 4.12)

5. NUMERICAL SIMULATIONS

5.1. Numerical methods. As in [17, 36] we consider the unit square with periodic boundary conditions as the domain for our numerical simulations if not stated otherwise. The particle system (1.3) is solved by either the simple explicit Euler scheme or higher order methods such as the Runge-Kutta-Dormand-Prince method, all resulting in very similar simulation results. Note that the time step has to be adjusted depending on the value of the cutoff radius R_c . For efficient numerical simulation we consider cell lists as outlined in [36].

5.2. Numerical results. Numerical results are shown in Figures 4, 5 and 6. For all numerical simulations we consider $N = 600$ particles which are initially equiangular distributed on a circle with centre $(0.5, 0.5)$ and radius 0.005 as illustrated in Figure 4(A). The stationary solution for linear force coefficients

$$f_s(|d|) = a_s|d| + b_s, \quad f_l(|d|) = 0.1 - 3|d|$$

for different values of a_s, b_s is shown in Figure 4. As proven in Section 4.1 equidistantly distributed particles along the vertical straight line form an unstable steady state for $N \in \mathbb{N}$ sufficiently large for $R_c \in (0, 0.5)$. Hence, the stationary solutions are no lines of uniformly distributed particles and we obtain different clusters or line patterns instead. In Figure 4(B), we consider $R_c = 0.3$, resulting in clusters of particles along the vertical axis. For $R_c = 0.5$ and a_s, b_s chosen as $a_s = -\frac{b_s}{R_c}$, the requirement in (4.19) for the necessary stability condition to be satisfied with equality, the real part of one of the eigenvalues of the stability matrix is equal to zero. The resulting steady states is shown for different scalings of the parameters a_s, b_s in Figures 4(C) and 4(D). One can see that the particles align along a vertical line along the entire interval $[0, 1]$, but are not equidistantly distributed along the vertical axis and thus the vertical straight line is an unstable steady state for any $N \in \mathbb{N}$ sufficiently large. For $a_s > -\frac{b_s}{R_c}$ and $a_s < -\frac{b_s}{R_c}$, respectively, with $R_c = 0.5$ the corresponding steady states are shown in Figures 4(E) and 4(F), resulting in clusters along the vertical axis.

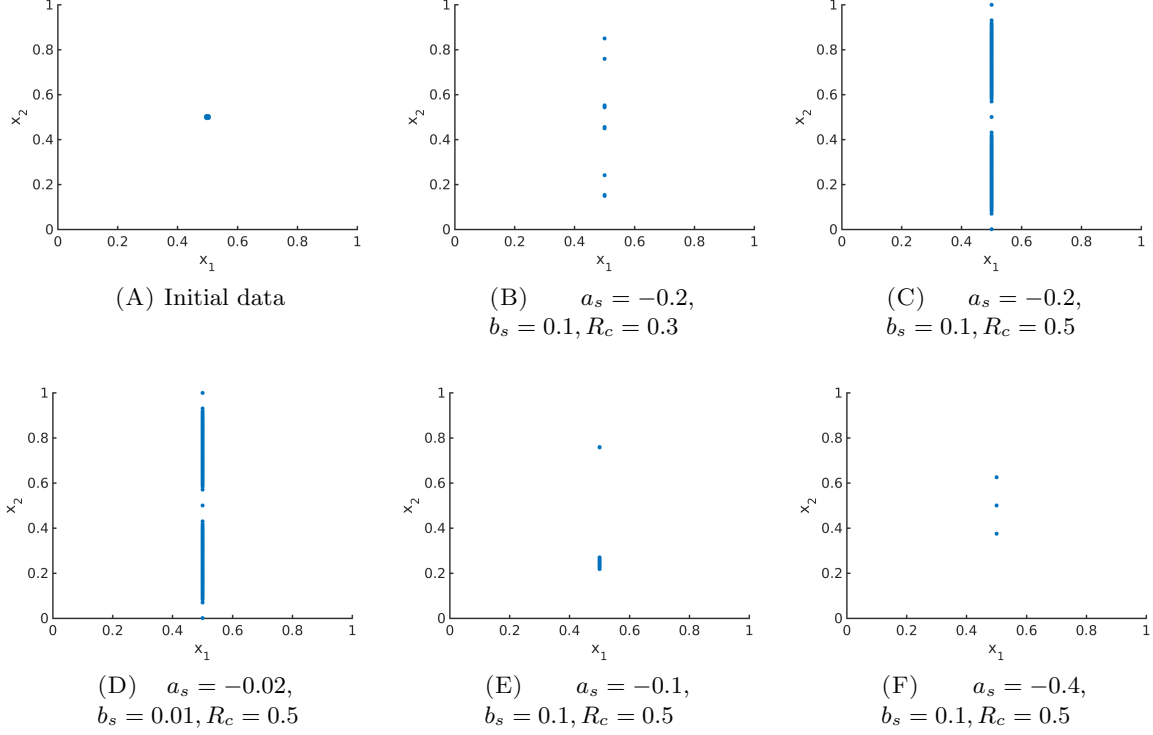


FIGURE 4. Stationary solution to the model (1.3) for total force (2.9) with linear force coefficients $f_l(|d|) = a_l|d| + b_l$, $f_s(|d|) = a_s|d| + b_s$ in (4.1) with $a_l = -3$, $b_l = 0.1$ and cutoff radius R_c

For an exponentially decaying force coefficient f_s along s , given by

$$f_s(|d|) = c \exp(-e_s|d|) - c \exp(-e_s R_c)$$

in (4.28), we consider the parameter values $c = 0.1$ and $e_s = 100$ if not stated otherwise and the initial data is given by equiangular distributed particles on a circle with centre $(0.5, 0.5)$ and radius 0.005 in Figure 5(A). As expected, for small values of e_s and $R_c \in (0, 0.5)$, e.g. $e_s = 10$ as in Figure 5(B), the equidistantly distributed particles along the vertical axis are an unstable steady state. In this case, the steady state is given by clusters along the vertical axis and $\Re(\lambda_2(m)) \leq 0$ for $m < 12$ only. For $R_c = 0.5$ the straight vertical line is stable as shown in Figure 5(C). Note that the additional constant in the definition of f_s leads to $f_s(R_c) = 0$ and is necessary for the stability of the straight vertical line. In Figure 5(D) we consider f_s without this additional constant, i.e. $f_s(|d|) = c \exp(-e_s|d|)$, where the straight vertical line is clearly unstable and we have $\Re(\lambda_2(m)) \leq 0$ for $m < 9$ only. If e_s is chosen sufficiently large, e.g. $e_s = 100$ as in Figures 5(E) and 5(F), the straight vertical line appears to be stable even for $R_c < 0.5$. An explicit calculation of the eigenvalues for $R_c = 0.1$ reveals, however, that $\Re(\lambda_2(m)) \leq 0$ for $m < 73723$ only. Note that we obtain stability for a much larger number of modes as in Figures 5(B) and 5(D). This is also consistent with a straight vertical line as steady state in Figure 5(F), while we have clusters as steady states in Figures 5(B) and 5(D). Further note that $\Re(\lambda_2(73723)) = 8.3225 \cdot 10^{-15}$ and hence it is numerically zero. As discussed in Remark 4.13 this explains why for $\exp(e_s R_c) \gg 1$, e.g. $e_s = 100$ and $R_c = 0.1$, the straight vertical line appears to be stable. Finally, we also obtain the straight vertical line as a steady state if we consider exponentially decaying force coefficients $f_l(|d|) = 0.13 \exp(-100|d|) - 0.03 \exp(-10|d|)$ instead of $f_l(|d|) = 0.1 - 3|d|$ as shown in Figure 5(F). Note that we also obtain a straight vertical line as

stationary solution in Figures 5(E) and 5(F) if $f_s(|d|) = c \exp(-e_s|d|) - c \exp(-e_s R_c)$ is replaced by $f_s(|d|) = c \exp(-e_s|d|)$ since $\exp(-e_s R_c) \ll 1$ for $e_s \gg 1$.

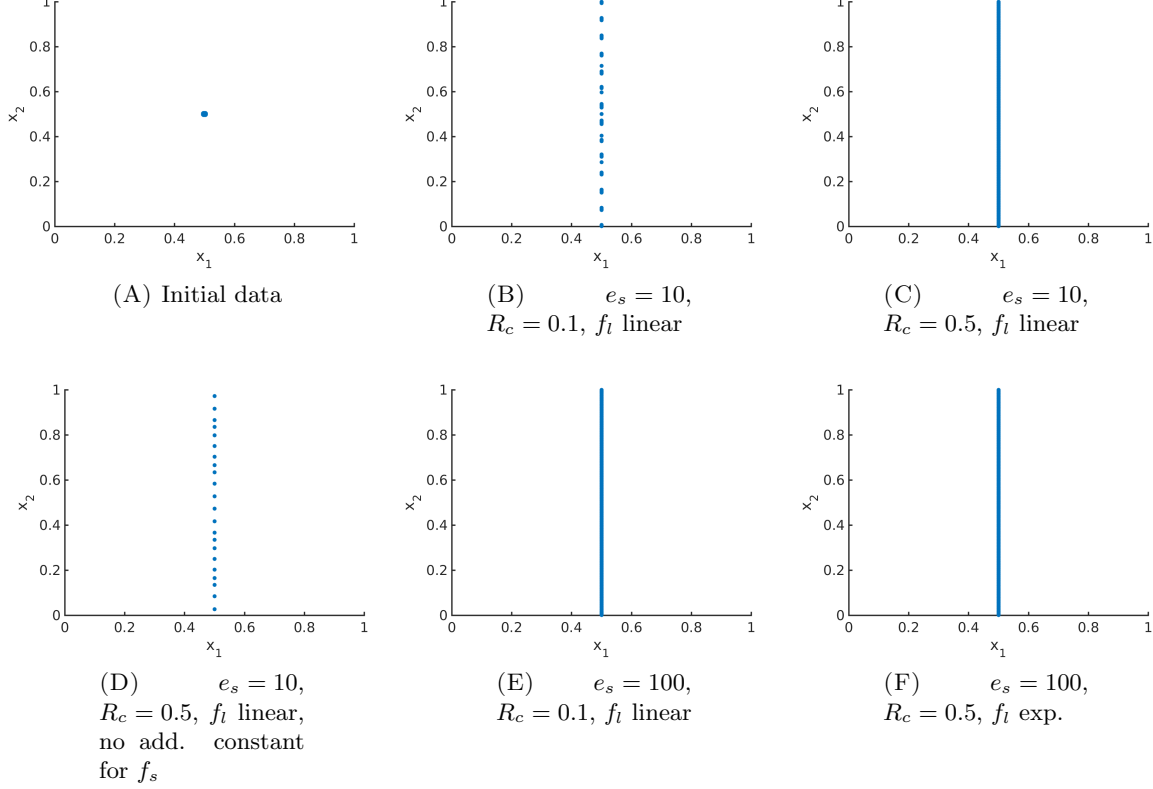


FIGURE 5. Stationary solution to the model (1.3) for total force (2.9) with exponential force coefficient $f_s(|d|) = c \exp(-e_s|d|) - c \exp(-e_s R_c)$ in (4.28) along s and $f_l(|d|) = 0.1 - 3|d|$ or $f_l(|d|) = 0.13 \exp(-100|d|) - 0.03 \exp(-10|d|)$ along l with cutoff R_c

In Figure 6 the stationary solution is shown on the domain $[0, 3]^2$ instead of the unit square. Here, we consider the same force coefficients as in Figure 5(F), i.e. exponentially decaying force coefficients along l and s . We define the initial data on $[0, 3]^2$ by considering the initial data on the unit square, i.e. equiangular distributed particles on a circle with centre $(0.5, 0.5)$ and radius 0.005, and extending these initial conditions to $[0, 3]^2$ by using the periodic boundary conditions. As expected we obtain three parallel lines as stationary solution.

ACKNOWLEDGEMENTS

JAC was partially supported by the EPSRC through grant number EP/P031587/1. BD has been supported by the Leverhulme Trust research project grant ‘Novel discretizations for higher-order nonlinear PDE’ (RPG-2015-69). LMK was supported by the UK Engineering and Physical Sciences Research Council (EPSRC) grant EP/L016516/1 and the German National Academic Foundation (Studienstiftung des Deutschen Volkes). CBS acknowledges support from Leverhulme Trust project on Breaking the non-convexity barrier, EPSRC grant Nr. EP/M00483X/1, the EPSRC Centre Nr. EP/N014588/1, the RISE projects CHiPS and NoMADS, the Cantab Capital Institute for the Mathematics of Information and the Alan Turing Institute.

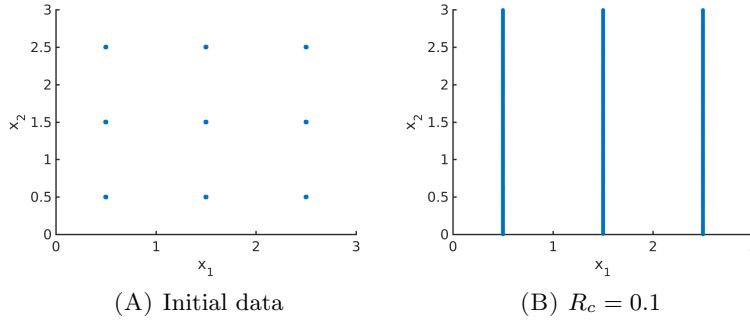


FIGURE 6. Stationary solution to the model (1.3) for total force (2.9) with exponential force coefficients $f_s(|d|) = c \exp(-e_s|d|) - c \exp(-e_s R_c)$ in (4.28) and $f_t(|d|) = 0.13 \exp(-100|d|) - 0.03 \exp(-10|d|)$ with cutoff R_c on the domain $[0, 3]^2$

REFERENCES

- [1] G. Albi, D. Balagué, J. A. Carrillo, and J. H. von Brecht. Stability analysis of flock and mill rings for second order models in swarming. *SIAM J. Appl. Math.*, 74(3):794–818, 2014.
- [2] L. A. Ambrosio, N. Gigli, and G. Savaré. *Gradient flows in metric spaces and in the space of probability measures*. Lectures in Mathematics. Birkhäuser, 2005.
- [3] D. Balagué, J. A. Carrillo, T. Laurent, and G. Raoul. Dimensionality of local minimizers of the interaction energy. *Archive for Rational Mechanics and Analysis*, 209(3):1055–1088, 2013.
- [4] D. Balagué, J. A. Carrillo, T. Laurent, and G. Raoul. Nonlocal interactions by repulsive-attractive potentials: radial ins/stability. *Physica D: Nonlinear Phenomena*, 260:5–25, 2013.
- [5] D. Balagué, J. A. Carrillo, and Y. Yao. Confinement for repulsive-attractive kernels. *Disc. Cont. Dyn. Sys.-B*, 19:1227–1248, 2014.
- [6] P. Ball. *Nature’s patterns: A tapestry in three parts*. Oxford University Press, 2009.
- [7] M. Ballerini, N. Cabibbo, R. Candelier, A. Cavagna, E. Cisbani, I. Giardina, V. Lecomte, A. Orlandi, G. Parisi, A. Procaccini, M. Viale, and V. Zdravkovic. Interaction ruling animal collective behaviour depends on topological rather than metric distance: evidence from a field study. *Proc. Natl. Acad. Sci.*, 105:1232–1237, 2008.
- [8] A. J. Bernoff and C. M. Topaz. A primer of swarm equilibria. *SIAM J. Appl. Dyn. Syst.*, 10:212–250, 2011.
- [9] A. L. Bertozzi, J. A. Carrillo, and T. Laurent. Blow-up in multidimensional aggregation equations with mildly singular interaction kernels. *Nonlinearity*, 22(3):683, 2009.
- [10] A. L. Bertozzi, T. Laurent, and F. Léger. Aggregation and spreading via the newtonian potential: The dynamics of patch solutions. *Mathematical Models and Methods in Applied Sciences*, 22(supp01):1140005, 2012.
- [11] A. L. Bertozzi, H. Sun, T. Kolokolnikov, D. Uminsky, and J. H. von Brecht. Ring patterns and their bifurcations in a nonlocal model of biological swarms. *Comm. Math. Sci.*, 13(4):955–985, 2015.
- [12] B. Birnir. An ode model of the motion of pelagic fish. *Journal of Statistical Physics*, 128(1):535–568, 2007.
- [13] A. Blanchet, V. Calvez, and J. A. Carrillo. Convergence of the mass-transport steepest descent scheme for the subcritical patlak–keller–segel model. *SIAM Journal on Numerical Analysis*, 46(2):691–721, 2008.
- [14] A. Blanchet, J. Dolbeault, and B. Perthame. Two-dimensional Keller-Segel model: Optimal critical mass and qualitative properties of the solutions. *Electronic Journal of Differential Equations (EJDE)*, 44:1–33, 2006.
- [15] S. Boi, V. Capasso, and D. Morale. Modeling the aggregative behavior of ants of the species *polyergus rufescens*. *Nonlinear Analysis: Real World Applications*, 1(1):163–176, 2000.
- [16] M. Burger, V. Capasso, and D. Morale. On an aggregation model with long and short range interactions. *Nonlinear Analysis: Real World Applications*, 8(3):939–958, 2007.
- [17] M. Burger, B. Düring, L. M. Kreusser, P. A. Markowich, and C.-B. Schönlieb. Pattern formation of a nonlocal, anisotropic interaction model. *Mathematical Models and Methods in Applied Sciences*, 28(03):409–451, 2018.
- [18] S. Camazine, J.-L. Deneubourg, N. R. Franks, J. Sneyd, G. Theraulaz, and E. Bonabeau. *Self-organization in biological systems*. Princeton Univ. Press, Princeton, 2003.
- [19] J. A. Cañizo, J. A. Carrillo, and F. S. Patacchini. Existence of compactly supported global minimisers for the interaction energy. *Archive for Rational Mechanics and Analysis*, 217(3):1197–1217, 2015.
- [20] J. A. Carrillo, M. G. Delgadino, and A. Mellet. Regularity of local minimizers of the interaction energy via obstacle problems. *Communications in Mathematical Physics*, 343(3):747–781, 2016.

- [21] J. A. Carrillo, M. Di Francesco, A. Figalli, T. Laurent, and D. Slepčev. Global-in-time weak measure solutions and finite-time aggregation for nonlocal interaction equations. *Duke Math. J.*, 156(2):229–271, 02 2011.
- [22] J. A. Carrillo, M. Di Francesco, A. Figalli, T. Laurent, and D. Slepčev. Confinement in nonlocal interaction equations. *Nonlinear Analysis: Theory, Methods and Applications*, 75(2):550–558, 2012.
- [23] J. A. Carrillo, L. C. F. Ferreira, and J. C. Precioso. A mass-transportation approach to a one dimensional fluid mechanics model with nonlocal velocity. *Advances in Mathematics*, 231(1):306–327, 2012.
- [24] J. A. Carrillo, M. Fornasier, J. Rosado, and G. Toscani. Asymptotic flocking dynamics for the kinetic cuckoo–smale model. *SIAM Journal on Mathematical Analysis*, 42(1):218–236, 2010.
- [25] J. A. Carrillo, M. Fornasier, G. Toscani, and F. Vecil. Particle, kinetic, and hydrodynamic models of swarming. In *Mathematical modeling of collective behavior in socio-economic and life sciences*, Model. Simul. Sci. Eng. Technol., pages 297–336. Birkhäuser Boston, Inc., Boston, MA, 2010.
- [26] J. A. Carrillo, Y. Huang, and S. Martin. Explicit flock solutions for Quasi-Morse potentials. *European J. Appl. Math.*, 25(5):553–578, 2014.
- [27] J. A. Carrillo, Y. Huang, and S. Martin. Nonlinear stability of flock solutions in second-order swarming models. *Nonlinear Anal. Real World Appl.*, 17:332–343, 2014.
- [28] J. A. Carrillo, F. James, F. Lagoutière, and N. Vauchelet. The filippov characteristic flow for the aggregation equation with mildly singular potentials. *Journal of Differential Equations*, 260(1):304–338, 2016.
- [29] J. A. Carrillo, R. J. McCann, and C. Villani. Kinetic equilibration rates for granular media and related equations: entropy dissipation and mass transportation estimates. *Revista Matemática Iberoamericana*, 19:971–1018, 2003.
- [30] J. A. Carrillo, R. J. McCann, and C. Villani. Contractions in the 2-wasserstein length space and thermalization of granular media. *Archive for Rational Mechanics and Analysis*, 179(2):217–263, 2006.
- [31] José A. Carrillo and Yanghong Huang. Explicit equilibrium solutions for the aggregation equation with power-law potentials. *Kinet. Relat. Models*, 10(1):171–192, 2017.
- [32] A. Cavagna, A. Cimarelli, I. Giardina, G. Parisi, R. Santagati, F. Stefanini, and R. Tavarone. From empirical data to inter-individual interactions: unveiling the rules of collective animal behavior. *Math. Models Methods Appl. Sci.*, 20, 2010.
- [33] P. Degond and S. Motsch. Large scale dynamics of the persistent turning walker model of fish behavior. *Journal of Statistical Physics*, 131:989–1021, 2008.
- [34] A. M. Delprato, A. Samadani, A. Kudrolli, and L. S. Tsimring. Swarming ring patterns in bacterial colonies exposed to ultraviolet radiation. *Phys. Rev. Lett.*, 87:158102, 2001.
- [35] M. R. D’Orsogna, Y. L. Chuang, A. L. Bertozzi, and L. S. Chayes. Self-propelled particles with soft-core interactions: Patterns, stability, and collapse. *Phys. Rev. Lett.*, 96:104302, 2006.
- [36] B. Düring, C. Gottschlich, S. Huckemann, L. M. Kreusser, and C.-B. Schönlieb. An Anisotropic Interaction Model for Simulating Fingerprints. arXiv:1711.07417, submitted, 2017.
- [37] L. Edelstein-Keshet, J. Watmough, and D. Grunbaum. Do travelling band solutions describe cohesive swarms? an investigation for migratory locusts. *J. Math. Bio.*, 36:515–549, 1998.
- [38] K. Fellner and G. Raoul. Stable stationary states of non-local interaction equations. *Mathematical Models and Methods in Applied Sciences*, 20(12):2267–2291, 2010.
- [39] K. Fellner and G. Raoul. Stability of stationary states of non-local equations with singular interaction potentials. *Mathematical and Computer Modelling*, 53(7–8):1436–1450, 2011.
- [40] R. C. Fetecau, Y. Huang, and T. Kolokolnikov. Swarm dynamics and equilibria for a nonlocal aggregation model. *Nonlinearity*, 24:2681–2716, 2011.
- [41] T. Kolokolnikov, J. A. Carrillo, A. Bertozzi, R. Fetecau, and M. Lewis. Emergent behaviour in multi-particle systems with non-local interactions [Editorial]. *Phys. D*, 260:1–4, 2013.
- [42] T. Kolokolnikov, H. Sun, D. Uminsky, and A. L. Bertozzi. Stability of ring patterns arising from two-dimensional particle interactions. *Phys. Rev. E*, 84(1):015203, Jul 2011.
- [43] M. Kücken and C. Champod. Merkel cells and the individuality of friction ridge skin. *Journal of Theoretical Biology*, 317:229 – 237, 2013.
- [44] H. Li and G. Toscani. Long-time asymptotics of kinetic models of granular flows. *Archive for Rational Mechanics and Analysis*, 172(3):407–428, 2004.
- [45] A. Mogilner and L. Edelstein-Keshet. A non-local model for a swarm. *J. Math. Biol.*, 38:534–570, 1999.
- [46] A. Mogilner, L. Edelstein-Keshet, L. Bent, and A. Spiros. Mutual interactions, potentials, and individual distance in a social aggregation. *Journal of Mathematical Biology*, 47(4):353–389, 2003.
- [47] A. Okubo and S. A. Levin. Diffusion and ecological problems. In *Interdisciplinary Applied Mathematics: Mathematical Biology*, page 197–237. Springer, New York, 2001.
- [48] J. K. Parrish and L. Edelstein-Keshet. Complexity, pattern, and evolutionary trade-offs in animal aggregation. *Science*, 284:99–101, 1999.
- [49] I. Prigogine and I. Stenger. *Order out of Chaos*. Bantam Books, New York, 1984.

- [50] G. Raoul. Non-local interaction equations: Stationary states and stability analysis. *Differential Integral Equations*, 25:417–440, 2012.
- [51] Robert Simione. *Properties of Minimizers of Nonlocal Interaction Energy*. ProQuest LLC, Ann Arbor, MI, 2014. Thesis (Ph.D.)—Carnegie Mellon University.
- [52] C. M. Topaz and A. L. Bertozzi. Swarming patterns in a two-dimensional kinematic model for biological groups. *SIAM J. Appl. Dyn. Syst.*, 65:152–174, 2004.
- [53] C. M. Topaz, A. L. Bertozzi, and M. A. Lewis. A nonlocal continuum model for biological aggregation. *Bull. Math. Biol.*, 68(7):1601–1623, 2006.
- [54] C. Villani. *Topics in optimal transportation*. Graduate studies in mathematics. American Mathematical Society, cop., Providence (R.I.), 2003.
- [55] J. H. von Brecht and D. Uminsky. On soccer balls and linearized inverse statistical mechanics. *Journal of Nonlinear Science*, 22(6):935–959, 2012.
- [56] J. H. von Brecht, D. Uminsky, T. Kolokolnikov, and A. L. Bertozzi. Predicting pattern formation in particle interactions. *Mathematical Models and Methods in Applied Sciences*, 22(supp01):1140002, 2012.